DEVELOPMENT AND CHARACTERISATION OF MAGNETICALLY RESPONSIVE AND ACTIVE AGENT LOADED ALGINATE BASED MICROSPHERES TO BE USED IN THE TREATMENT OF HEPATOCELLULAR CARCINOMA (HCC)

HEPATOSELLÜLER KARSİNOM (HSK) TEDAVİSİNDE KULLANILMAK ÜZERE MANYETİK ALANA DUYARLI VE ETKEN MADDE İÇEREN ALJİNAT BAZLI MİKROKÜRELERİN GELİŞTİRİLMESİ VE KARAKTERİZE EDİLMESİ

ŞÜKRAN ALPDEMIR

PROF. DR. EMİR BAKİ DENKBAŞ

Supervisor

Submitted to the Graduate School of Science and Engineering of Hacettepe University

as a Partial Agreement to the Requirements for the Award of the Degree of Masters of Science in Bioengineering

2019

This work titled "**Development and Characterisation of Magnetically Responsive and Active Agent Loaded Alginate Based Microspheres to be Used in the Treatment of Hepatocellular Carcinoma (HCC)**" by **ŞÜKRAN ALPDEMIR** has been approved as a thesis for the Degree of **Master of Science** in **Bioengineering** by the Examining Committee Members mentioned below.

Prof. Dr. Ahmet ÇABUK
Head

Prof. Dr. Emir Baki DENKBAŞ
Supervisor

Prof. Dr. Mustafa TÜRK
Member

Prof. Dr. Lokman UZUN
Member

Assist. Prof. Dr. Batur ERCAN
Member

This thesis has been approved as a thesis for the Degree of **Master of Science in Bioengineering** by Board of the Directors of the Institute of Graduate School of Science and Engineering on ……/…../……

Prof. Dr. Menemşe GÜMÜŞDERELİOĞLU
Director of the Institute of
Graduate School of Science and Engineering

ETHICS

In this thesis study, prepared in accordance with the spelling rules of Institute of Graduate Studies in Science of Hacettepe University,

I declare that

- all the information and documents have been obtained in the base of the academic rules
- all audio-visual and written information and results have been presented according to the rules of scientific ethics
- in case of using other Works, related studies have been cited in accordance with the scientific standards
- all cited studies have been fully referenced
- I did not do any distortion in the data set
- and any part of this thesis has not been presented as another thesis study at this or any other university

29/01/2019

ŞÜKRAN ALPDEMİR

YAYIMLAMA VE FİKRİ MÜLKİYET HAKLARI BEYANI

Enstitü tarafından onaylanan lisansüstü tezimin/raporumun tamamını veya herhangi bir kısmını, basılı (kağıt) ve elektronik formatta arşivleme ve aşağıda verilen koşullarla kullanıma açma iznini Hacettepe Üniversitesine verdiğimi bildiririm. Bu izinle Üniversiteye verilen kullanım hakları dışındaki tüm fikri mülkiyet haklarım bende kalacak, tezimin tamamının ya da bir bölümünün gelecekteki çalışmalarda (makale, kitap, lisans ve patent vb.) kullanım hakları bana ait olacaktır.

Tezin kendi orijinal çalışmam olduğunu, başkalarının haklarını ihlal etmediğimi ve tezimin tek yetkili sahibi olduğumu beyan ve taahhüt ederim. Tezimde yer alan telif hakkı bulunan ve sahiplerinden yazılı izin alınarak kullanması zorunlu metinlerin yazılı izin alarak kullandığımı ve istenildiğinde suretlerini Üniversiteye teslim etmeyi taahhüt ederim.

Yükseköğretim Kurulu tarafından yayınlanan ***"Lisansüstü Tezlerin Elektronik Ortamda Toplanması, Düzenlenmesi ve Erişime Açılmasına İlişkin Yönerge"*** kapsamında tezim aşağıda belirtilen koşullar haricince YÖK Ulusal Tez Merkezi/H.Ü. Kütüphaneleri Açık Erişim Sisteminde erişime açılır.

☐ Enstitü / Fakülte yönetim kurulu kararı ile tezimin erişime açılması mezuniyet tarihimden itibaren 2 yıl ertelenmiştir.

☐ Enstitü / Fakülte yönetim kurulu gerekçeli kararı ile tezimin erişime açılması mezuniyet tarihimden itibaren .... ay ertelenmiştir.

☐ Tezim ile ilgili gizlilik kararı verilmiştir.

25/02/2019

ŞÜKRAN ALPDEMİR

ABSTRACT

DEVELOPMENT AND CHARACTERISATION OF MAGNETICALLY RESPONSIVE AND ACTIVE AGENT LOADED ALGINATE BASED MICROSPHERES TO BE USED IN THE TREATMENT OF HEPATOCELLULAR CARCINOMA (HCC)

Şükran ALPDEMİR

Master of Science, Department of Bioengineering

Advisor: Prof. Dr. Emir Baki Denkbaş

January 2019, 83 pages

Today, cancer is the foremost common and deadly disease in the world. One of the most important cancer types is liver cancer and occurs either by being directly involved with liver cells resulting in primary liver cancers, or by the metastasis of other cancer cells originating from different organs and reaching the liver second-hand, thus resulting in secondary liver cancer. Among the liver cancer types, especially in the primary liver cancers, the cancer type named hepatocellular carcinoma (HCC) plays the largest part and is considered to be a global health problem worldwide. Whether for the new HCC cases occurring every year or for the fact that it makes up a considerable part of diseases resulting in death, HCC has currently been divided into three fundamental stages: early, middle, and advanced. While surgical intervention or ablation can have a high success rate when treating HCC in its early stage, for patients at the middle stage transarterial characterization and chemoembolization

(TACE) procedures provide both a better success in treatment and a prolonged life regiment. Within the scope of the presented thesis, a chemoembolization agent, containing a new generation drug and imaging agent used in TACE applications, is to be developed which can be visualised using a magnetic resonance imaging (MRI) machine. For this purpose, the development and evaluation of microspheres in clinical applications carried out by in vitro tests, especially of alginate based polymer structures combined with appropriate antineoplastic agents (such as Sorafenib) is the aim of this project. Additionally, super paramagnetic iron oxide nanoparticles (SPIONs), which were synthesized for the purpose of MRI imaging and therefore tracking the microspheres during the treatment process, were tested for their potential in use during treatment via hyperthermia.

Keywords: Hepatocellular Carcinoma (HCC), Transarterial Chemoembolization (TACE), Super Paramagnetic Iron Oxide Nanoparticles (SPIONs), Alginate microspheres, Sorafenib, Hyperthermia treatment

ÖZET

HEPATOSELLÜLER KARSINOM (HSK) TEDAVISINDE KULLANILMAK ÜZERE MANYETIK ALANA DUYARLI VE ETKEN MADDE İÇEREN ALJINAT BAZLI MIKROKÜRELERIN GELIŞTIRILMESI VE KARAKTERIZE EDILMESI

Şükran ALPDEMİR

Yüksek Lisans, Biyomühendislik

Tez Danışmanı: Prof. Dr. Emir Baki Denkbaş

Ocak 2019, 83 sayfa

Kanser hastalıkları günümüzde tüm dünya genelinde en yaygın ve en ölümcül hastalıkların başında gelmektedir. Kanser hastalıklarının en önemli gruplarından birini de karaciğer kanserleri oluşturmaktadır. Karaciğer kanserleri ya doğrudan karaciğer hücreleri aracılığı ile primer karaciğer kanserleri olarak meydana gelmekte ya da diğer organlarda başlayan kanser oluşumlarının metastaz yaparak karaciğer sekonder olarak ulaşmasıyla karaciğer kanserine dönüşmektedirler. Karaciğer kanserleri arasında özellikle primer kanserlerde hepatosellüler karsinom (HSK) adı verilen (Hepatocellular Carcinom, HCC) kanser türü en büyük paya sahip olan kanser grubudur ve halihazırda tüm dünya genelinde, global bir sağlık sorunu olarak değerlendirilmektedir. Gerek her yıl görülen yeni vaka olarak ve gerekse ölüme sebep olan hastalıklar arasında oldukça önemli yer tutan HSK temel başlangıç, orta ve ileri evre şeklinde kabaca gruplandırılabilen üç temel evreye sahiptir. Başlangıç evresinde cerrahi

müdahale ve ablasyon gibi tedavilerde yüksek oranda başarı elde edilirken orta evrede yer alan hastalarda transarteriyel katerizasyon ile kemoembolizasyon (TAKE) (transarterial chemoembolization, TACE) uygulamaları gerek başarılı tedavi ve gerekse yaşam süresini uzatmaya yönelik tedavi rejimlerini oluşturmaktadır. Sunulan tez kapsamında TAKE uygulamalarında kullanılan yeni nesil ilaç ve görüntüleme ajanı taşıyan manyetik rezonas (MR) görüntüleme ile yönlendirilebilen kemoembolizasyon ajanı geliştirilmesi planlanmaktadır. Bu amaçla özellikle aljinat bazlı polimer yapıları ile uygun antineoplastik ajanları (Sorafenib gibi) ile kombine tedavilerde kullanılabilecek mikroküreleri geliştirilmesi ve in vitro testleri yapılarak klinik uygulamalara hazırlık şeklinde değerlendirmelerin yapılması hedflenmiştir. Ek olarak, MRI görüntüleme potansiyeli bulunan ve böylece tedavi sürecinde mikroküreleri takip edebilecek süper paramanyetik demir oksit nanoparçacıkları (SPION'lar), hipertermi yoluyla tedavi sırasında kullanım potansiyelleri açısından test edildi.

Anahtar Kelimeler: transarteriyel katerizasyon ile kemoembolizasyon (TAKE), süper paramanyetik demir oksit nanoparçacıkları (SPION'lar), hipertermi, Sorafenib, manyetik rezonas (MR)

ACKNOWLEDGEMENTS

Firstly, I would like to sincerely thank my supervisor, Prof. Dr. Emir Baki Denkbaş who has always supported and encoured me through-out my studies with enthusiasm, immense knowledge and suggestions and help throughout the research development and documentation of this work. I want to express my profound acknowledgment and deep thanks to the additional help and support that I received from Assist. Prof. Tayfun Vural who has always been there whenever I was stuck and needed help, for assistance in the lab while running experiments, for research design, and for analysis of experimental results and from Research Assistant Göknur Kara for being available at any time to answer any of my questions or any time I needed help during the research and experimental process.

I thank my parents father Mahmut Nedim and mother Rabia, brothers Ibrahim and Yusuf, and grandmother Hafize for trusting in me completely, being my indispensable support, who have lived through this process right along with me, and whom I aim to make proud.

A very special gratitude goes to my friends Amina and Izgen for giving me support along the way.

I thank my fellow labmates in Biopolymeric Systems Research Group (BSRG) who were a joyful part of this long sweet-sour journey; Soheil Malekghasemi, Ebru Erdal, Zeynep Karahalilioğlu, Eda Yalçın, Ebru Kılıçay, Gizem Daban, Betül Bozdoğan Pala, Öznur Akbal, Serhat Öztürk, Ekin Çelik and Ali Örs.

Last but not least, I thank my work colleagues and friends in TUBITAK and my head of department Prof. Dr. Selda Ulutas for always giving their support and making the process so much easier.

CONTENTS

LIST OF TABLES

LIST OF FIGURES

LIST OF ABBREVIATIONS AND SYMBOLS

SPIONs	Super Paramagnetic Iron oxide nanoparticles
HCC	Hepatocellular Carcinoma
VSM	Vibrating sample magnetometer
ESR	Electron Spin Resonance
PDI	Polydispersion index
TACE	Transarterial Chemoembolization

1. INTRODUCTION

Today, cancer continues being one of the deadliest diseases in the world. Although Cancer Research is one the most popular research areas in the medical sciences area, the full mechanisms of the disease, and thus curing it, still alludes the many bright minds carrying out the research. In addition to being deadly, cancer can invade the body very swiftly and silently. The fact that many different types of cancers exist, does not help the situation.

Among the many different types of treatments, chemotherapeutic agents are the most popular among doctors. The disadvantage of this treatment type is that chemotherapy is very difficult to target only on to the cancer cells and thus affect the healthy cells too, making the patient's situation and quality of life while getting the treatment, so much worse. To counteract this problem, targeted drug delivery methods have been developed and continues to be further perfected.

One of the deadliest cancers is Hepatocellular carcinoma (HCC) and is more commonly known as Liver cancer. It is the 3rd most common cancer that causes death and results in one million deaths annually, globally. It can arise from cirrhosis and other liver diseases that are chronic and can be classified as a primary malignancy [1]. The beginning cell(s) of this cancer is thought to arise from hepatic stem cells, this however is still not fully proved. The spreading of the tumours occurs in three ways, these are: distant metastasis, expansion in the local region, and intrahepatic spreading [1].

HCC is most commonly seen in Asia and Africa, due to the high predominance of hepatitis B and C occurring in these regions. These liver diseases can then be the primary stimuli for chronic liver diseases to emerge, and afterwards, for HCC development. It is presumed that the cases of HCC will steadily increase as time goes by [2]. As HCC mostly forms in the presence of a cirrhotic liver, a treatment known as Orthotopic Liver Transplantation (OLT) has been found to be one of the best effective options for both the chronic liver disease and HCC. However, as most HCC patients are at later stages of the disease, this treatment method is not suitable for them [3, 4].

For patients at an intermediate stage of HCC, a common treatment that is being currently used, is Trans-Arterial Chemoembolization (TACE). For patients to be able to receive TACE

as a treatment, they must have either a single large nodule of more than 5 cm in size, compensated liver failure, or multifocal HCC with no breaching into any vascularity or any additional hepatic spreading. The reason as to why TACE is the preferred treatment method when it comes to intermediate stage HCC is due to the fact that the survival rate of patients was found to be higher in contrast to the finest palliative care or to substandard therapies [5]. In a study carried out by Llovet et al, a meta-analysis of 6 randomized controlled trials was conducted where TACE was compared with the finest palliative care or substandard therapies that could be used for HCC treatment. Nevertheless, significant heterogeneity existed between the designs of the individual studies (of which the technique of TACE and the patient populations were also included), in addition to the study results, with only two of the six individual studies reporting 2-year survival with a statistically significant improvement in survival rate when compared to moderate treatments. It has been reported that 15-62% of patients were found to have partial responses, an average advancement in survival rate of 16-20 months and the progression of the tumour slowing down significantly [6].

Even though TACE is now a conventional method that is widely used as mentioned before for the treatment of HCC at an intermediate-stage, patients at this stage of cancer consist of a wide range and thus the same amount of success rates are not observed between them. Therefore, Drug Eluting Bead - Trans-Arterial Chemo Embolization (DEB-TACE) is now preferred and repetitive applications of TACE are also administered. However, these repetitive applications can increase negative symptoms associated with TACE applications and thus careful precautions should be taken, such as how the patient's response was to the first TACE application, any previous liver diseases existing, or if the tumour has developed and how much.

For a model application of DEB-TACE the encapsulating particle that encompasses the chemotherapeutic drug should allow a slow release which should be continuously maintained in the targeted tumour without affecting other parts of the body in addition to the embolization of the blood supplying vessels of the tumour. Although lipoidol has previously been exploited for this purpose due to hepatocellular carcinoma cells being very compatible with them, it was found that slow release of the drug and a constant concentration was not maintained [5].

Recently, a new method that greatly helps with the disadvantages of lipoidol microspheres has been developed. This method consists using microspheres for the purpose of embolization that can collect doxorubicin hydrochloride out of a solution actively, and secrete it slowly and continuously thereby decreasing the secretion of the chemotherapeutic agents to other parts of the body and subsequently increasing the drug concentrations in the tumour regions and making treatment much more efficient [5]. Additionally, microspheres that have embolic properties have also been developed recently and studies have shown that they are, in fact, able to actively take-up chemotherapeutic drugs from a solution and, via controlled release, significantly decrease the levels of drugs entering the circulation as opposed to ethiodized oil-based applications [5].

A disadvantage of TACE and DEB-TACE is that efficient and good imagery cannot be provided as, currently, CT scans are usually used [7]. This is also not beneficial to the patient as they are subjected to radio waves every time an image of the treatment process is to be taken and this further increases health hazards towards the patient. This study aims to prevent this disadvantage by using Magnetic Resonance Imagery (MRI) which can relatively reduce these negative factors as it uses a magnetic field to produce a much more accurate image, an easier way to carry out a prognosis, and a much safer imaging technique for the patient as it does not have the health hazards that CT scans pose. Additionally, by encapsulating Super Paramagnetic Iron Oxide Nanoparticles into the alginate microspheres, hyperthermia studies will be carried out so that the microspheres can be sent to the tumour region much more accurately by an external magnetic field and, in addition to chemotherapeutic agent release, the SPIONs will give of a particular excitation by applying energy and heat up inside the tumours, thus destroying them internally. This method combined with chemotherapy will be more effective in the treatment of hepatocellular carcinoma.

2. GENERAL INFORMATION

2.1 Liver Anatomy and Physiology

Understanding the anatomy and physiology of the liver is very important when it comes to finding methods for curing liver diseases, especially when it comes to cancer, more specifically hepatocellular carcinoma. Therefore, before going in to more detail in the thesis, a brief overview of the anatomy and physiology of the liver will be covered. Thus, it will be easier to visualize what is being carried out in this thesis and what improvements can be made in the future. Thus, in this chapter, the anatomy will first be covered with the physiology of the liver included in the next section.

2.1.1 Gross Anatomy:

The liver is situated on the right side extending towards the kidney, below the diaphragm. It has a right-angled triangular shape and covers the majority of the abdominal cavity. The kidney is surrounded by connective tissues and is made up of soft tissues that are of a brown-light reddish colour. The connective tissue mesh encircling the liver is further surrounded and made stronger by the peritoneum found in the abdominal cavity thus holding it in place and guarding it from any damage.

The liver is attached to the peritoneum by four areas. These are: the falciform, the coronary, and the triangle shaped right and left ligaments. Even though these attachments are called ligaments, they are not in the true sense anatomically so. In fact, they are compressed areas of the peritoneal membrane holding up the liver.

The liver is made up of four separate lobes. These are the quadrate, right, caudate, and right lobes [8].

- There is a ligament called the falciform ligament which divides the right from the left lobes, which are also the biggest lobes, with the right lobe being five to six times bigger than the left lobe which becomes gradually even smaller at one end.
- Circling the inferior vena cava is the caudate lobe which is also small and reaches from the latter part of the right lobe.
- The quadrate lobe is also small and also reaches from the latter end of the right lobe and encircles the gallbladder.

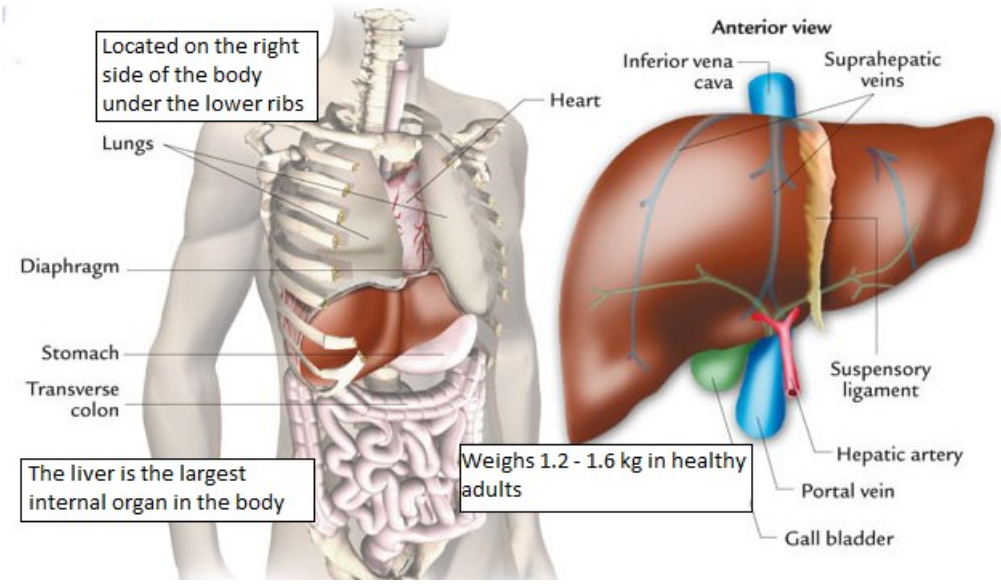

Figure 2.1 The situation of the liver in the body [9]

2.1.1.2 Blood Vessel System:

The hepatic portal vascular system is a one-of-a-kind blood supply system that is special for the liver. The blood supply of the liver is unique among all organs of the body due to the hepatic portal vein system. The hepatic portal vein is the meeting point of blood entering from the capillary vessels of the pancreas, spleen, gallbladder, intestines, and stomach. This blood is then sent to the liver which “cleans” it by separating it into smaller blood vessels and re-sending the cleaned blood back into the blood circulation. For the blood to be sent to the rest of the body, it must first be sent to the heart. This is done via the blood collecting in the veins of the liver and being sent to the vena cava and subsequently to the heart. For the oxygenation of hepatocytes, the liver’s own arterioles and arteries supply blood that has been oxygenated [8].

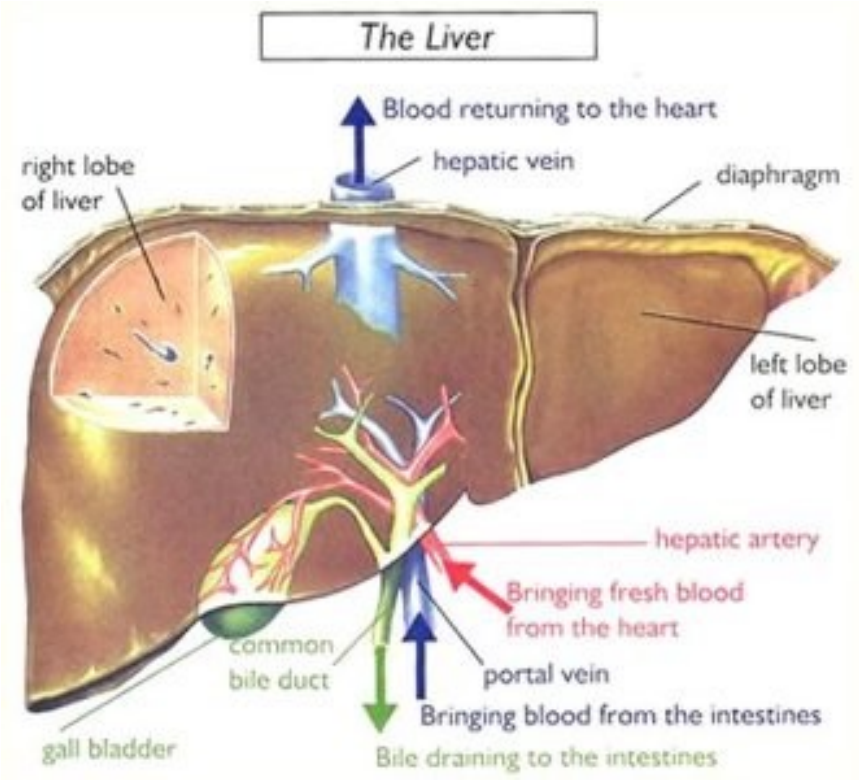

Figure 2.2 Liver anatomy [10]

2.1.2 Physiology

2.1.2.1 Digestion

For digestion, bile is needed which is synthesized by the liver. The composition of bile consists of cholesterol, water, bile salts, and the bilirubin pigment. After bile is synthesized by the liver cells, it is passed on to the gall bladder where it is stored and can be released when needed. Bile is usually needed for the digestion of fats which, once the fatty foods arrive at the duodenum, the cholecystokinin hormone is secreted so that bile can be discharged from the gallbladder and subsequently reach the duodenum via bile ducts. Once the bile reaches the fats, they become emulsified thus decreasing them into smaller sizes with larger surface area for the body to more easily digest as it is normally harder when in larger masses [11].

When red blood cells have run their course in the body, they become unable to carry out their function properly and become worn out and must therefore be removed. Their removal also occurs in the liver. The liver contains Kupffer cells which can take the old red blood cells from the blood stream, dismantle them and send them to the hepatocytes. Here,

haemoglobin can easily be digested into its components, heame and globin. However, the heame group poses a problem. It contains iron and this makes it indigestible by the body and so gets converted into bilirubin which is then mixed in with the bile and excreted from the system. Bilirubin is a coloured pigment which gives the greenish hue to bile. In fact, bilirubin is also the reason why patients with liver diseases have a more yellowish tinge in their skin, as bilirubin accumulation can occur in these patients [8, 11].

2.1.2.2 Metabolism

One of the liver's main jobs is the metabolism of substances like lipids, carbohydrates, and proteins and turn them into products that can be used by the body. For this to be feasible, the liver is situated in the body so that all the blood leaving the digestive system must flow through the hepatic portal vein and subsequently pass through the hepatocytes of the liver.

When it comes to the digestion of carbohydrates, they are firstly split into glucose which is the monomer of carbohydrates and is the main energy supply for the cells in the body. Glucose is stored as glycogen by the hepatocytes which also convert the glucose contained in the blood entering from the hepatic portal vein into this macromolecule. The structure of glycogen allows the quick reconversion and release of glucose by hepatocytes when needed, such as when food is not being eaten. This is called homeostasis and helps to regulate a balanced blood sugar level at all times in the body.

The metabolism of fatty acids also is needed for the production of energy and this is carried out by converting them into ATP. This process also occurs in the hepatocytes of the liver. To do this, hepatocytes transform glycerol, which is a lipid, into glucose by a process known as gluconeogenesis and lipids such as lipoproteins, cholesterol, and phospholipids are also synthesized by hepatocytes. Most cholesterol is also mixed in as a substance of bile and discharged by the body along with it.

For proteins that are taken in from the diet, they are first metabolized into their amino acid monomers by the digestive system after which they are sent to the liver via the hepatic portal vein. For amino acids to be utilized as energy producing molecules, they first have to have their amine groups taken away and converted into ammonia and, subsequently, urea as it is less dangerous and can be easily discharged from the body via urine. Finally, the leftover amino acid parts can then be converted into ATP or go through gluconeogenesis and result in glucose production [8].

2.1.2.3 Detoxification

The blood can have many toxic substances in it that have to be removed before they can spread to the whole of the body due to blood circulation. This detoxification job also befalls on to the liver. The blood is first checked by the liver hepatocyte cells once they arrive via the hepatic portal vein and the substances that can pose as a danger to the body, like drugs and alcohol, are broken down to non-dangerous substances and subsequently excreted out of the system. Additionally, to maintain homeostasis, blood hormone levels must also be kept within limits and thus the liver can break down and take away hormones that are secreted by glands in a person's own body [8].

2.1.2.4 Storage

The liver is also essential for the storage of many important substances needed by the body. These include vitamins like A, D, E, K, and B12, and minerals like copper and iron, so that a continual contribution of these substances are available for the body when needed. Additionally, fatty acids are also stocked in hepatocytes obtained from the metabolism of triglycerides. Furthermore, after the conversion of glucose, which arrives in the liver cells due to insulin stimuli, into glycogen, this polysaccharide can also be stored and used for the maintenance of a continual level of blood glucose via homeostasis. This storage of essential components that are important for survival is made possible due to the hepatic portal system, through which there is a constant blood circulation [8].

2.1.2.5 Synthesis

The synthesis of essential parts of proteins also occur in the liver. These parts include albumin, fibrinogen, and prothrombin parts. These proteins are essential for keeping the internal environment of the body constant and preserve the balance needed for a person to keep their health. While the proteins fibrinogen and prothrombin play roles in the clotting of blood, albumin proteins are involved in osmoregulation by preserving blood isotonic environment and preventing an increase or decrease of water content in cells during times of abnormal levels of fluid in the body [8].

2.1.2.6 Immunity

The liver, until recently, was not known for having any role in immunity. However, studies carried out in the near past have proven that not only is the liver involved in immunity but

that has a significantly important role in the process. As is known, the liver is made up of a number of specialized cells that result in the liver having a multitude of important roles in the regulation of the substances in the body via homeostasis and the metabolism and removal of harmful substances. One of these cells are the Kupffer cells which are situated along the sinusoidal structure of the liver. These specialized cells allow the liver to play a role in the immune system. Kupffer cells are a part of the innate immune system and their close situation to the non-parenchymal and parenchymal cells of the liver allows them to easily control liver function in health as well as in disease. They, in addition to spleen and lymph node macrophages, belong to the system of mononuclear phagocytes. Their job consists of binding and excreting out substances like glycol-proteins, foreign substances, bacteria, parasites, lysosomal enzymes, parasites, old red blood cells, fungi, and viruses. Therefore, keeping the Kupffer cells working optimally is very important as this can lead to the taking over of pathogens or systemic inflammation or both. However, stimulation of Kupffer cells when there is a liver diseases involved can also result in unwanted symptoms like unrestrained inflammation of the liver [12].

As a summary, the main jobs the liver performs in the body are as follows:

- The liver can synthesize energy instantaneously
- The synthesis of proteins for the purpose of repairing tissue, development of body
- The accumulation of sugars, minerals, and vitamins to be used for numerous necessary functions
- The controlling of the transferring of fat to different areas of the body
- Blood coagulation regulation
- The controlling of the amount of blood drug and chemical levels
- The controlling of hormone levels and keeping them balanced
- Bile synthesis to assist with digestion
- The excretion of cholesterol when their levels are at a surplus
- Getting rid of toxic substances
- Alcohol digestion
- An important organ for the production of blood before a baby is born
- Assists in preventing infection
- Renewing damaged tissues of itself

- The eradication of bacteria from the blood system and thus helping to prevent infections
- The excretion of excrements and thus cleaning the blood

2.2 Hepatocellular Carcinoma and How It Arises

As stated before, hepatocellular carcinoma (HCC) gives rise to approximately 1 million deaths yearly, world-wide. There are probably certain pathological factors that result in HCC being specific to certain age, geography, and gender distribution. While liver cancer is the fifth commonest cancer found and the 2nd in cancers that result in death in men, it is the seventh commonest cancer found to be diagnosed and 6th in cancer related deaths in women, world-wide. This cancer was also observed in children, albeit at much lower proportions of 0.05 diagnoses per one hundred thousand children for 2009 in the US. The yearly observance of HCC in 2010 in the US was 6 cases per one hundred thousand [13, 14].

The diagnosis rate of HCC is approximately identical to the death rate of this disease world-wide, and this signifies the danger of this cancer type. Hepatitis C and B infections that are chronic make up 80% of HCC incidence cases [15].

As previously stated, liver cancer prevalence was mostly observed in Asian and African countries. However, evidence shows that the death rate and prevalence rate is now spreading to many areas worldwide, with central Europe, North America, and Latin America being amongst the countries with the highest increases observed. According to the National Cancer Institute Surveillance, Epidemiology and End Results (SEER) Database of the National Cancer institute in the United States, the occurrence rate of liver cancer showed an annual increase of 3.1% between the years 2008 and 2012. It was also observed that liver cancer prevalence was three times higher in men than in women (with men having 11.5 incidence rates per one hundred thousand as compared to 3.9 for women). In this time period, the occurrence rate of HCC was found to become higher in non-Hispanic blacks and whites, and Native Americans/Alaskans, while a decrease was observed in Pacific Islanders and non-Hispanic Asians which could be attributed to the increasing amount of vaccinations carried out against Hep B infections in children. When compared with the decrease observed in deaths in other cancers like prostate, lung, and breast cancers, there was an increase of 2.8% yearly for men and 3.4% for women. These data show that the threat of HCC is very eminent and more emphasis in research for this cancer should be given [16, 17].

To understand hepatocellular carcinoma (HCC) more thoroughly, the underlying biology should be better explained. HCC results from cirrhosis and chronic liver disease that pre-existed before the cancer development. As stated previously, without being fully proved, it is thought that the source of HCC cells can come from hepatic stem cells after which the tumour can spread in three ways. These are distant metastasis, spreading within the liver, and local growth [18].

In the past decades, important developments in HCC incidence have been recorded. While HCC used to be diagnosed at much later stages, when symptoms like weight loss, pain in the upper-right area, and signs of liver loss of functions were observed, now diagnosis occurs at a much earlier stage due to regular screening and tests carried out on patients that present evidence of having cirrhosis, utilizing techniques that allow imaging of the body to appear cross-sectional (like MRI, CT, PET, and SPECT scans) and measurements carried out by AFPs (serum alpha-fetoproteins) [18].

There are a number of reasons as to why the incidence rate of HCC is believed to increase in the future. One of these reasons is the fact that the highest occurrence rate of HCC due to HCV (hep C virus) infection has not been reached yet. Another reason is the increasing occurrence rate of cirrhosis and it developing when NASH (non- alcoholic steatohepatitis) or NAFLD (non-alcoholic fatty liver disease) already exists in the area. The growth of NASH mostly occurs if the patient has one or a combination of the following disorders: diabetes (type 2), obesity, hypertension, and dyslipidemia. The fact that an increase in obesity rate continues to occur raises the risk of this disease with passing time. Therefore, producing better care that is more relevant and efficient for later and intermediate stage HCC is becoming ever more important [19, 20].

Even though incision of part of the liver may be beneficial for some patients, this may be a short-term answer to the problem [18]. In fact, most of the patients would most probably require organ transplanting for their liver as their stage of HCC would mostly be at a later stage when diagnosed and thus be ineligible for resection. However, given the extreme shortage of liver donations around the world, including developed countries, this is also a very limited choice of treatment. Therefore, relatively newer treatment methods like using chemoembolization agents, new chemotherapeutic drugs, RFA (radiofrequency ablation),

and local ablation treatments may increase patient life expectancy and provide better palliative conditions [21].

HCC pathological physiology is still not fully understood due to multiple factors affecting the formation and development of the cancer. When Beasley was able to find a relationship between the hepatitis B virus and HCC incidence in 1981, it was thought that the source of HCC development was determined. Later studies, however, did not fully prove this theory as many different hidden but present cirrhotic liver diseases, which were at the same time chronic, resulted in HCC development, even though some of these patients did not even test positive for HBV and had the DNA of HBV combined into the genome of the hepatocyte cells [18].

Livers with cirrhotic diseases have particular characteristics which subsequently result in HCC, including, fibrosis, inflammation, necrosis, and continuous regeneration. Patients who do not have cirrhosis diseases and may have a chance of HCC development but have hepatitis B virus infections, their liver may already have fibrosis and may have signs of regeneration. While patients that have HCV infections, develop HCC only if cirrhosis pre-exists [18]. This may be due to HBV being a virus based on combining its DNA into the genome of the host resulting in the production of a Hepatitis B Virus X protein which could be a major factor in HCC incidence. On the other hand, HCV is a virus that uses RNA replication which occurs in the cytoplasm of the host cell and therefore does not combine with the cell's DNA [18].

The development of the disease, which ultimately results in the tumour transforming into a malignant form, can be changed by the involvement of environmental and outside factors that finally result in changes genetically preventing apoptosis happening at the right time and escalating the proliferation of the tumour cells (the figure below is a depiction of this process) [18].

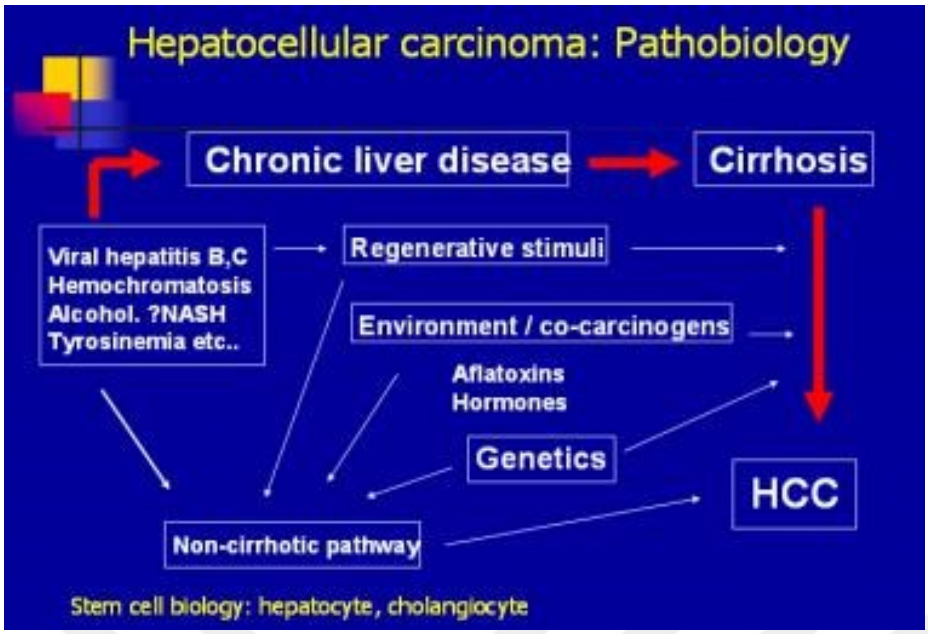

Figure 2.3 Hepatocellular carcinoma: pathobiology [18].

Understanding the genetic pathways involved in the formation of HCC is also essential for finding the most effective treatments for it. Research on this front has yielded some important findings. It was found that β-catenin, p53, and PIKCA genes may be essential in the process of HCC carcinogenesis as these were found to show the highest rate of mutations in hepatocellular carcinoma patients. However, more research needs to be conducted to find the signalling pathways affected that inevitably result in unrestrained division of hepatocellular carcinoma cells. It was discovered that there are some repeatedly changed pathways in HCC that control the differentiation of cells. Two of these pathways are the Hedgehog and the WNT- β-catenin pathways, and it was determined that the WNT pathway's upregulation resulted in an increase in transforming cells into malignancies as they were involved with preneoplastic adenomas [18, 22].

2.2.1 HCC Treatment with the Drug Sorafenib

In addition to the pathways mentioned above, another pathway known as the Ras-mitogen-activated protein kinase (MAPK) signalling pathway is involved (Figure 2.5) [23, 24]. This pathway is the one that controls the differentiation, increase, and endurance to live of the cancer cells. The mechanisms of the pathway start with the Ras protein which is situated in the cytosol and starts the series of successive reactions stimulated the product of each previous reaction (in other words a cascade), and the proteins involved are the kinase protein

Raf, the kinase protein MAPK (MEK), and ERK (or extracellular signal regulated kinase) [23, 25].

The role that Sorafenib, a bi-aryl urea molecule which prevents a number of kinase proteins, plays in the treatment of HCC is by blocking the receptors for tyrosine kinase proteins and delay the workings of the serine and threonine kinase proteins' mechanism occurring intracellularly to a later stage in the Ras/MAPK reaction cascade. The receptors which bind the kinase proteins known as tyrosine and are blocked by sorafenib are VEGFR-2 (vascular endothelial growth factor receptor), VEGFR-1, VEGFR-3, FLT-3, c-KIT, PGDFR, and RET. C-RAF, mutant B-RAF, and wild type B-RAF are also blocked. These proteins all instigate cancer cell angiogenesis and increase in number [26]. The figure below depicts the chemical structure of sorafenib.

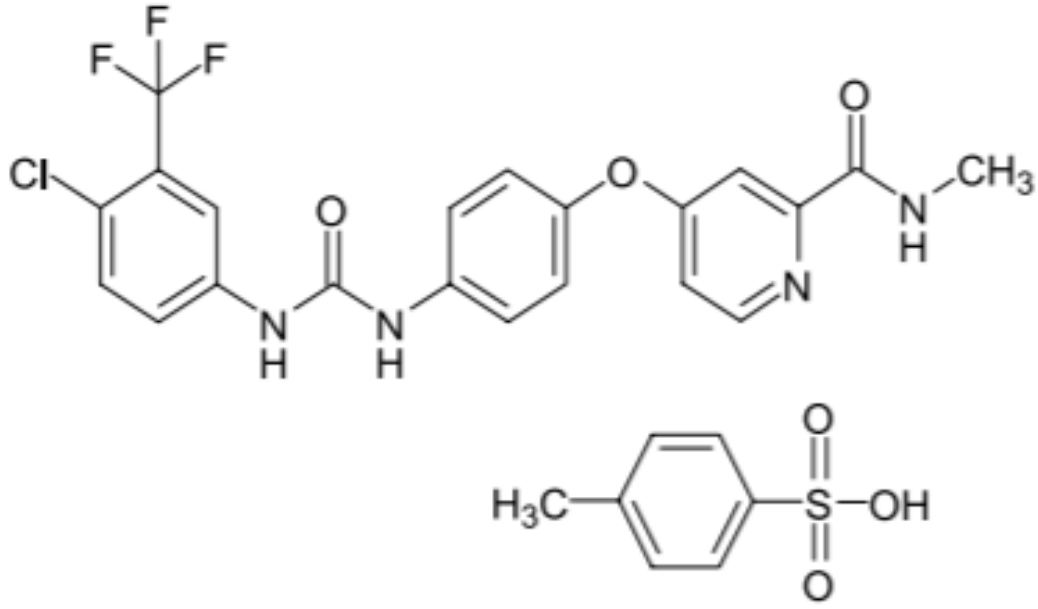

Figure 2.4 The chemical structure of the drug Sorafenib Tosylate [27]

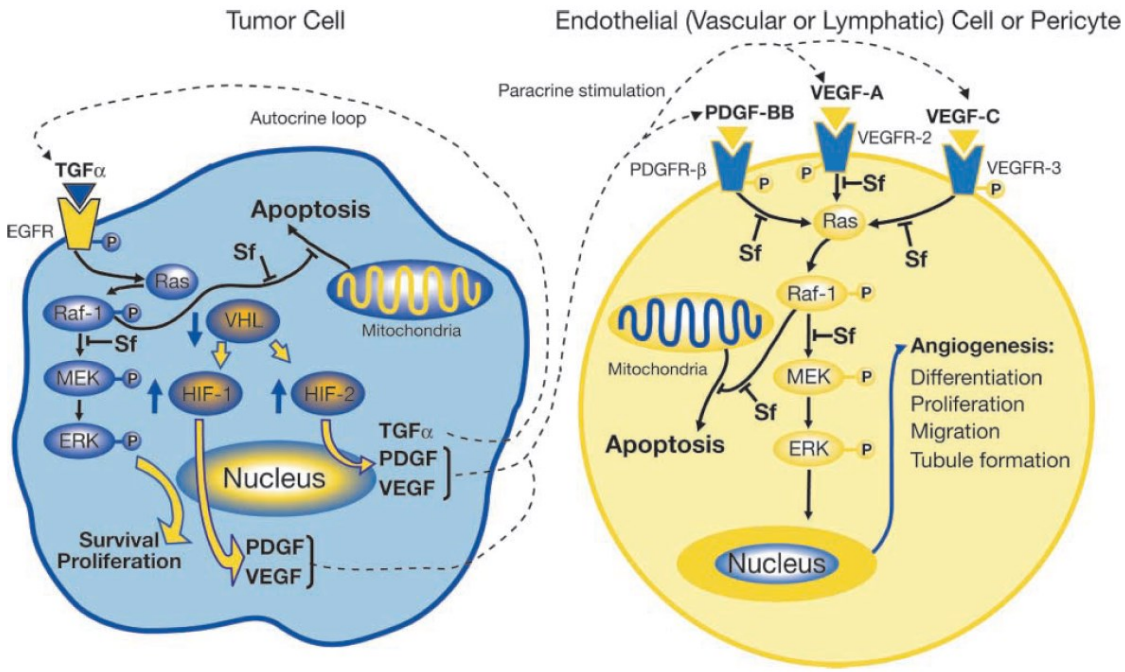

Figure 2.5. A disruption in signalling via Raf-1 in cells of the endothelial, tumour, and/or pericytes may result in the development of tumour cells and/or angiogenesis via an autocrine structure [24].

2.3 Controlled Drug Release Systems

To make treatment with drugs more efficient, the release of these drugs should be at optimal rates. Thus, designing optimal controlled release systems for drugs are essential for this purpose, and these designs may vary according to the drug being used. Controlled drug release systems allow the drug to be released steadily thus increasing the exposure time to the drug of the area to be treated, to prevent the drug from being disposed of too quickly, and to target the drug to the site of interest in the body without exposing it to other parts of the body as much as possible. It can also increase the standard of living of the patient as it will decrease the number of times the drug will be taken by them and could also increase the worth of the drug itself by lengthening patent protection. Lastly, the effects of different drugs could become more homogenous by using these systems. This last advantage is particularly relevant today, due to the increasing importance being given to the quality of the designs as opposed to the importance given to the quality of the tests as was in the past [28].

To make these aims a reality, one must first understand the mechanisms involved in controlled release systems and how to design them according to the application that is to be

used. For example, will the drug be administered orally, through the skin, regionally delivered, or delivered via targeted delivery to specific areas of the body using nanoparticles and what are the mechanisms involved for these applications? To answer these questions in relation to this thesis, the different mechanisms involved will first be divulged. The following mechanisms are involved in these applications and their involvements vary according to the methods of application: erosion, diffusion, partitioning, osmosis, swelling, dissolution, and targeting. The drug delivery method that was developed for the purpose of this thesis encompasses regional drug delivery combined with specific targeting using super paramagnetic iron oxide nanoparticles trans arterial catheters. The mechanisms involved in these methods rely on the disintegration of the polymer encapsulating the drug slowly but steadily, the swelling of the encapsulating polymer (alginate microspheres in this case), and the diffusion and dissolution of the drug from the pores of the microcapsule [28, 29].

There are two types of controlled release systems that is relevant to this study. These are embolization agents and chemoembolization agents. These will be discussed in more detail below.

2.3.1 Embolization Agents

In theory, this treatment method involves the blocking of blood vessels that provide nourishment from the blood circulation system of the body to the tumour cells. This then results in the cells' starvation and subsequently their death. This method relies on only the physical blockage of the vessels, the stimulation of platelets, and/or the stimulation of the blood clotting mechanism in the body. There are several agents that can be used for this purpose, all having different characteristics and utility and can be partitioned into two main groups: permanent, and temporary embolization agents. Permanent embolization is more effective for cancerous tumours.

Another important consideration for this method is the degree of blockage and the place. Embolization can be done in the arterioles or capillaries, or they can be done at a much more immediate site. This degree of embolization is dependent on the situation of the tumour, its location, and its progress. Additionally, the advancement in micro-catheter technology allows flexibility when wanting to deliver the embolization agents to much smaller and proximal vascular areas [30-32].

2.3.2 Chemoembolization Agents

The process of chemoembolization is very similar to embolization, except with the added advantage of using chemotherapeutic agents in addition to embolization agents. This results in both the blockage of the blood supply to the tumour and the necrosis of the tumour cells by the anticancer drug used at the site of administration. Thus, it is the merging of two processes together: chemotherapy and embolization. This procedure is usually used to treat HCC and is non-surgical, making it a much less invasive treatment method. The treatment technique used for HCC is known as Trans-Arterial Chemotherapy (TACE) (Figure 5), as was discussed before in previous chapters. This process will be talked about in more detail in the section below[32, 33].

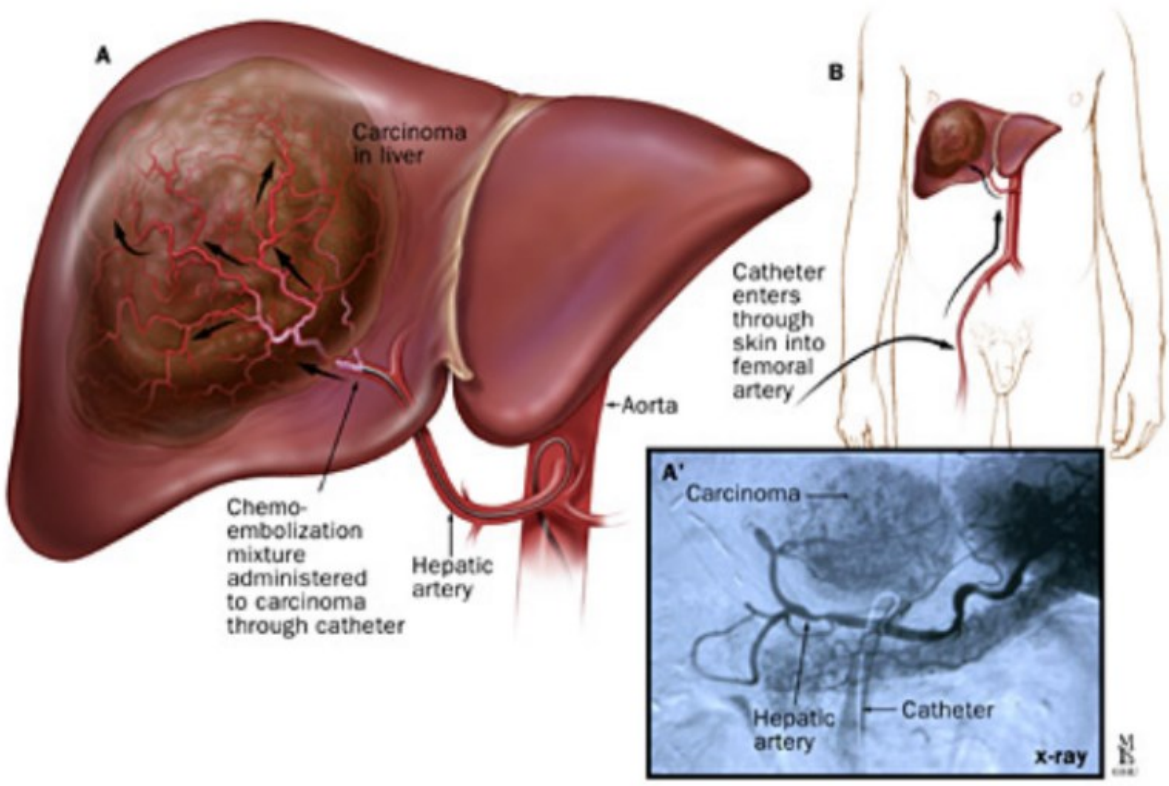

Figure 2.6. Depiction of how trans-arterial chemoembolization is carried out [34]

2.3.2 Trans-Arterial Chemoembolization (TACE)

A standard TACE procedure is made up of 2 steps. The first step is the sending of the chemotherapeutic agents into the blood vessel feeding the cancer cells by using a catheter placed within the artery. The second step constitutes the blocking of the blood vessel feeding

the tumour specifically via embolization. As mentioned in the chapter discussing the liver physiology, the liver has an uncommonly seen blood supply system supplied via two blood vessels, from which 2/3rd of the blood supplied comes via the hepatic portal vein and 1/3rd comes from the hepatic artery. Thus there will be minimal complications of sending the chemotherapeutic agents before blocking the hepatic artery, which provides the blood supply to the HCC tumour cells, and subsequently resulting in their death. Previously, embolic agents such as PVA particles, gelatine sponges, particles constituted of polymers, and biodegradable microspheres made up of starch have been used. TACE provides the ability to specifically target the treatment to the tumour in concentrated doses, preventing the healthy nearby cells from being affected. Additionally, embolization of the arteries supplying nourishment to the tumour cells provide a longer drug exposure time as it will be harder for the drugs to wash out because of the blockage [6, 33, 35].

Recently, it was found that incorporating the drug into the embolization agent, thus making it a carrier, was found to be more efficient and a better method. These particles would be injected directly into the site of interest and thus remove the need for a two-step procedure. These carriers were named as drug-eluting beads, or DEBs for short [33, 35]. This thesis concentrates on the development of a different type of microsphere as an embolization agent encapsulating a chemotherapeutic drug. These different TACE methods are illustrated in the figure below.

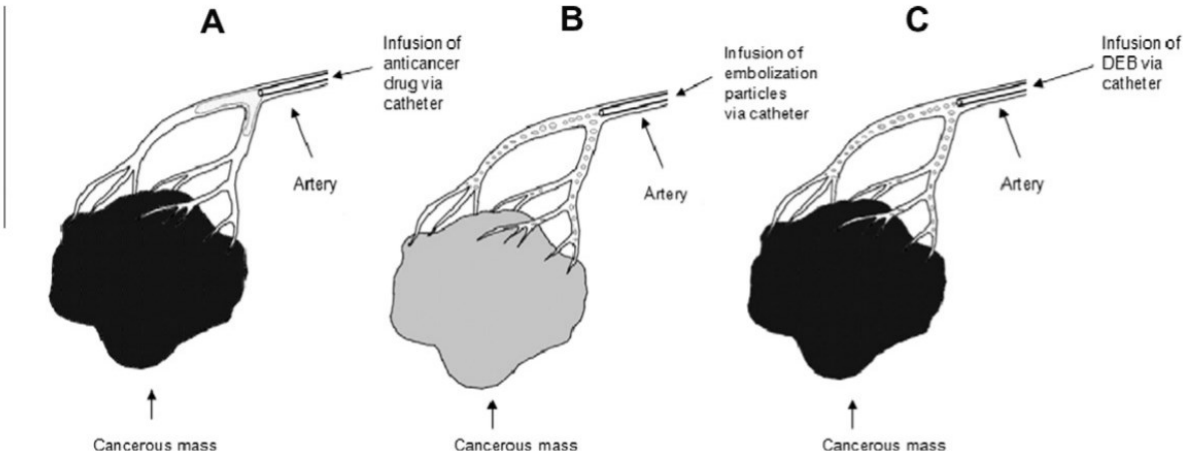

Figure 2.7. Different TACE methods showing (A) embolization using only chemotherapy, (B) embolization using only embolic agents, and (C) embolization using chemoembolization agents in the form of drug eluting beads (DEBs)[33]

2.4 Properties and Applications of Alginate for Targeted Drug Delivery Systems

Alginate is found in the cell walls of brown algae and exist as alginic acid salts, such as calcium alginate, magnesium alginate, and sodium alginate. The salt that is most commonly used is sodium alginate as it is the only alginate salt that can easily dissolve in water, and can usually be found as a white powder due to the various alterations the alginate salt goes through while being extracted.

Alginate is made up of two residues and exists in the form of linear copolymers. The monomers that make up this family of copolymers are β-D-mannuorate (M) and α-L-guluronate (G) which exist in blocks. These blocks can contain successive G residues (e.g. GGGGGG), successive M residues (e.g. MMMMMM), as well as varying M and G residues (e.g. GMGMGM) [36].

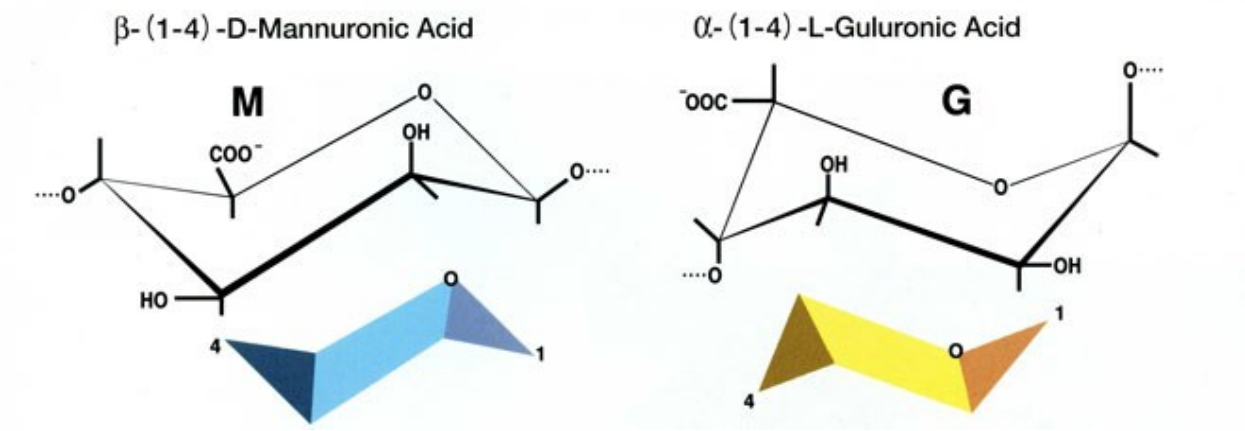

Figure 2.8. Chemical structures of the monomers that make up Alginate [37]

Alginate obtained from different sources have different chemical structures and properties due to different concentrations and lengths of G and M blocks in their structures. For example, bacterial alginate obtained from Azotobacteria are stiffer when in a gel form because of the higher concentration of G-blocks in its polymer structure [1]. Thus, the source from which the alginate is manufactured from plays an important role when utilizing alginate for various purposes. It is also believed that for hydrogel production, only G-blocks effect intermolecular cross-linking with divalent cations (e.g. Ca^{2+}). Therefore, M/G ratio, sequence, G-block length, and molecular weight all are important factors effecting the

physical properties of alginates and consequently the hydrogels produced from them. Currently more than two hundred different alginates are being produced commercially [36].

By increasing or decreasing the length of the G-blocks and the molecular weight of alginate, the mechanical properties can also be adjusted. For example, increasing the length of the G-blocks and the molecular weight of the alginate improves its mechanical properties. These adjustments then result in positive effects on alginate gel stability, drug release, and the phenotype and function of the cells encapsulated with-in the gel. Although, using a HMW (high molecular weight) alginate polymer increases the viscosity of the alginate solution produced and this is not preferred in procedures. An example of the disadvantage of this is when cells or proteins are incorporated into the alginate solution and, due to the shear force resulting from stirring and implanting into the body, they could get injured. Changing the molecular weight and how they are dispersed will allow the management of the solution before getting gelled and the stiffness after gelation. By mixing low and high molecular weighted polymers of alginate it is possible to increase elastic modulus without increasing the viscosity too much.

Single charged cations, when mixed with alginate, result in dissolvable salts. Double or more charged cations on the other hand (Mg^{2+} is an exception) result in the formation of precipitates or gels. Different compatibilities can be observed between alginate and different cations. This results in the development of gels showing ionotropy and is based on ionic binding selectively. Gels which are more concentrated can be obtained by using alginate with a higher concentration of G block residues as they have a higher compatibility to divalent ions when compare to alginate with a higher concentration of M block residues. The mannuronate/guluronic acid ratio is very effective when developing alginate gels as it affects their transmittance, their viscous and elastic properties, and their swelling properties. The most commonly used, and therefore most commonly studied, are the gels produced by using calcium chloride as a cross-linker. Additionally, alginate has the ability to form both acidic gels and gels with an equal distribution of charges (ionotropy) thus resulting in advantage over macromolecules that are only neutral. The process by which alginate gels release drugs is by swelling, thus this swelling property and its physical and chemical properties are determined by the gel type produced. The products of alginate, e.g. gels, are invaluable for drug delivery and other applications in medicine due to their non-toxic nature and that they are relatively biocompatible [36, 38, 39].

2.5 Magnetic Resonance Imaging and Hyperthermia

Hepatocellular carcinoma can be classified based on the progression of disease as stages as in all cancer diseases. In cancer detection, if we can catch the cancer disease at an earlier stage, a phenomena called early diagnosis, it can facilitate and increase the success ratio of the cancer therapy. In cancer diagnosis and therapy, the metastasis mechanism is one of the most important and critical stages of the cancer due to the difficulties in reaching the eradication of the cancer disease by the treatment. Therefore, the diagnosis of the cancer at a very early stage is the most effective parameter. This means that if the cancer can be detected at the earliest stage possible, it can be classified as an early diagnosis and can facilitate the cancer therapy and increase the success ratio of the therapy itself as previously mentioned [40-42].

The disease detection is possible in HCC as in all cancer diseases with radiological imaging techniques such as the ultrasonography (US) technique, computed tomography (CT), magnetic resonance imaging (MRI) and positron emitted tomography (PET) etc. and various serological markers [4]. The US technique has been determining the presence of intrahepatic lesions for around 40 years [43]. In fact, according to related literature the sensitivity of the US technique has changed from 35 to 83 % approximately while the specificity is larger than 90 % in screening studies [44, 45]. On the other hand, both sensitivity and specificity capabilities of the technique depends on the lesion structure and dimensions [46, 47]. In the case of CT and MRI lesions of smaller sizes can be detected with higher sensitivity and specificity in HCC diseases [48].

In literature, there are some studies related to using CT for HCC detection which was carried out using various microspheres and the microspheres were shown to give excellent visualisation under the X-ray in CT scans. Unfortunately, in CT which is an X-ray imaging technology has some potential radiation hazard. Due to this disadvantage of CT, MRI technology is preferred in the medical imaging diagnosis field. Here in MRI studies system can track the embolic agents where located in the body precisely on real time [49-53]**.** Additionally, MRI prevents the patient from the radiation hazard risks present when using the CT [54]. Nowadays during the MRI applications, researchers use superparamagnetic iron oxide nanoparticles (SPIONPs) as an additive into the embolic or chemo-embolic agents to result in enhanced MRI visualisation.

The Most well-known SPIONs are magnetite (Fe_3O_4) and maghemite (γ-Fe_2O_3) which have been widely used in diverse biomedical applications such as MRI contrast agents, bio-catalysis, biological separation, bio-sensing, diagnostic medical devices and hyperthermia [55-59]. In fact, hyperthermia is a physical therapy and when the SPIONs are exposed to an external magnetic field they generate heat and consequently kill the cancer cells [59-61]. In hyperthermia therapy, SPIONs can effectively destroy the cancer cells while keeping the normal cells if they can be hosted in the tumour region. Therefore, most probably hyperthermia can be considered as one of the most popular cancer therapy method in the near future. As the fundamental phenomena, the cancer cells are more sensitive to heat than normal cells [62, 63]. Therefore, when a high temperature (approximately 42.5°C) is applied around the tumour tissue region, the cells cannot release the heat energy via the blood flow due to the malfunctioned nature of the blood vessels [64]. The application procedure of embolization and hyperthermia for HCC is shown in Figure 2.9.

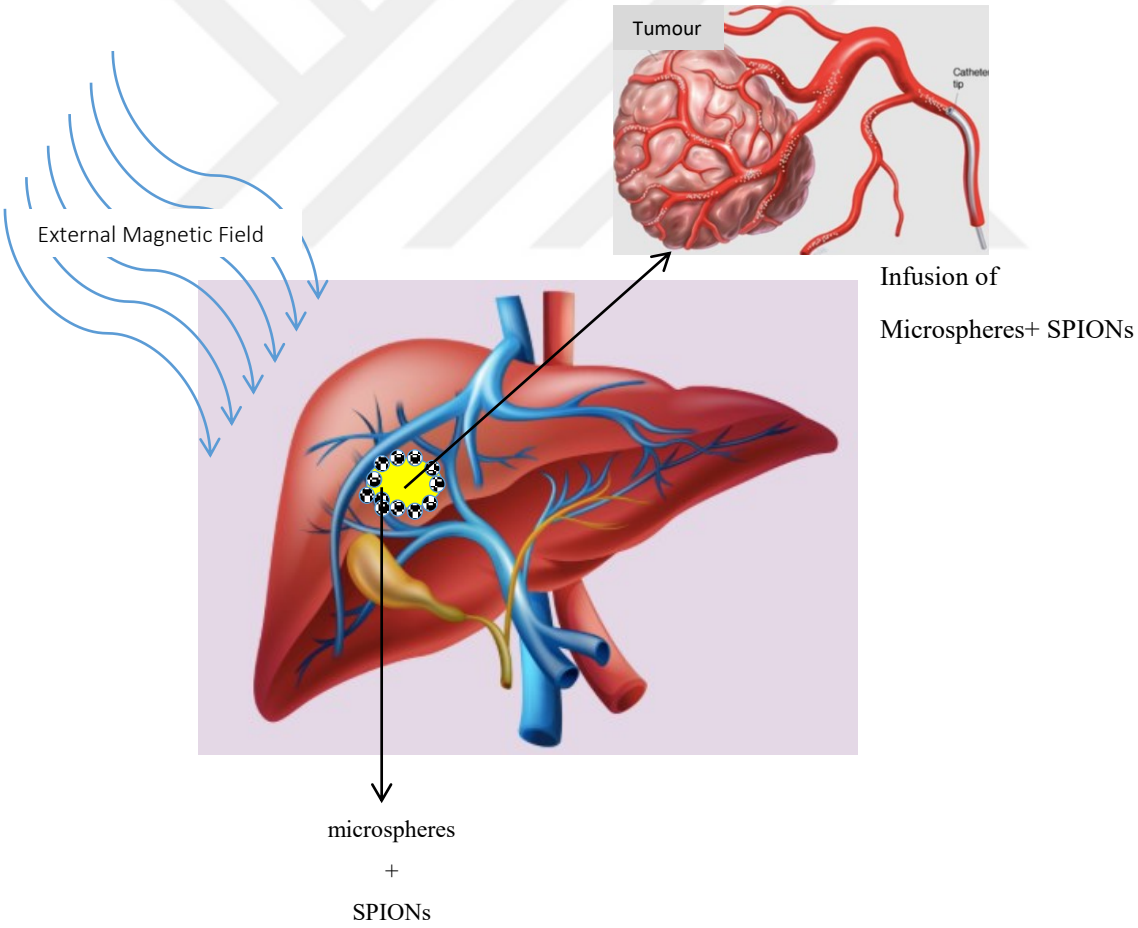

Figure 2.9. Hyperthermia and chemoembolization with SPION loaded microspheres

3. EXPERIMENTAL STUDIES

3.1 Chemicals

For the development of alginate microsphere; sodium alginate (Sigma Aldrich), Calcium Chloride (Sigma Aldrich), Tween-85 (Sigma Aldrich), and Hydroxypropyl Methylcellulose (HPMC) (Sigma Aldrich) were used. For the synthesis of Magnetic Iron Oxide nanoparticles; $FeCl_2.4H_2O$ Iron (II) Chloride (Merck, Germany), $FeCl_3.6H_2O$ Iron (III) Chloride (Merck, Germany), HCl (Merck, Germany), NaOH (Sigma Aldrich) were used while under a flow of nitrogen gas. As the chemotherapeutic agent, Sorafenib tosylate (Novartis) was used. dH2O was also used throughout all the procedures.

3.2 Alginate microsphere development

Alginate microbeads were found to be ideal agents for chemoembolization drug delivery systems for hepatocellular carcinoma, due to their biocompatibility and ease of production and usage. Therefore, alginate has also been used in this study. Until today, various methods for alginate bead formation were used. The most commonly used method has been the oil-in-water emulsification method. One important aim of the study, was to produce alginate microbeads that could easily be dried without too much loss of shape or change in size. This is important for mass production of the alginate microbeads and their ease of storage. In the oil-in-water emulsification method the sodium alginate solution was dispersed in an immiscible phase and congealed to form calcium alginate microspheres by reacting with calcium chloride. The method used in this study also is loosely based on this technique. The sodium alginate solution was dripped in to the Calcium chloride cross-linker solution that also included a surfactant. After the microspheres formed in the calcium chloride solution, they were left there for a significant amount of time and were then further hardened by isopropyl alcohol. It was found that the size, shape and surface characteristics of the microspheres formed were markedly affected by the stirring speed, rate of addition of sodium alginate into the calcium chloride solution and concentration and composition of the encapsulating and crosslinking solutions [38, 65-67]. One non variable was the equipment used for the production of the micro-bead shapes themselves. Here the Buchi Encapsulator B-395 Pro was used. The Buchi Encapsulator B-395 Pro provided the opportunity to tune various variables like frequency, flow rate of the alginate droplets into the crosslinking

solution via the pumping speed of the syringe, electric voltage, stirring rate, and the nozzle size out of which the alginate microspheres were dropped from so that the ideal shaped and sized calcium alginate microspheres could be used.

Briefly, the ideal concentrations of the sodium alginate solution (the encapsulant) and calcium chloride solution (the cross linker) were determined by using the optimization method, where there was only one variable and the other parameters were constants. As the smallest sized microspheres were aimed for, the smallest sized nozzle for the encapsulator was used throughout the experiments. This nozzle size was of 80 µm and was a non-variable parameter. One other non-variable was the electric voltage (around 600mV) as this was found to be constant for the 80um nozzle. The variable parameters were as follows: CaCl2 solution concentration, sodium alginate concentration, frequency, flow rate.

Preparation of the CaCl2 solution as cross-linker was as follows: seven different CaCl2 concentrations were prepared. These were 0.1%, 0.5%, 1%, 1.5%, 3%, 5%, and 10%. For each run, 100 ml of the calcium chloride solution was prepared. The table below shows the different formulations and frequencies applied.

Table 3.1. Different parameters tested for obtaining optimal sized and shaped Alginate microspheres

Calcium Chloride Concentration	Frequency	Electric Voltage	Size of nozzle
0.1%	1400 Hz	600 mV	80 um
0.1%	1600 Hz	600 mV	80 um
0.1%	1800 Hz	600 mV	80 um
0.5%	1400 Hz	600 mV	80 um
0.5%	1600 Hz	600 mV	80 um
0.5%	1800 Hz	600 mV	80 um
1%	1400 Hz	600 mV	80 um
1%	1600 Hz	600 mV	80 um

1%	1800 Hz	600 mV	80 um
1.5%	1400 Hz	600 mV	80 um
1.5%	1600 Hz	600 mV	80 um
1.5%	1800 Hz	600 mV	80 um
5%	1400 Hz	600 mV	80 um
5%	1600 Hz	600 mV	80 um
5%	1800 Hz	600 mV	80 um
10%	1400 Hz	600 mV	80 um
10%	1600 Hz	600 mV	80 um
10%	1800 Hz	600 mV	80 um

The process of encapsulation by the Buchi Encapsulator relies on the Plateau-Rayleigh Instability, or the Rayleigh Instability as it is better known, which gives an understanding of how droplets form from a continuous flowing stream of liquid and how these droplets have the same volume even with a lower surface area. The area of fluid dynamics that this phenomenon is based on is related to the separation into smaller droplets of a fluid stream thread and is linked to the Rayleigh-Taylor instability. This instability has been utilized in machinery like the encapsulator so that a constant stream of fluid in droplet form can be formed by perturbation. This instability works due to the fact that liquids decrease their surface area because of existing tension in their surface. The schematic representation of how the encapsulator works can be seen in figure 3.1.

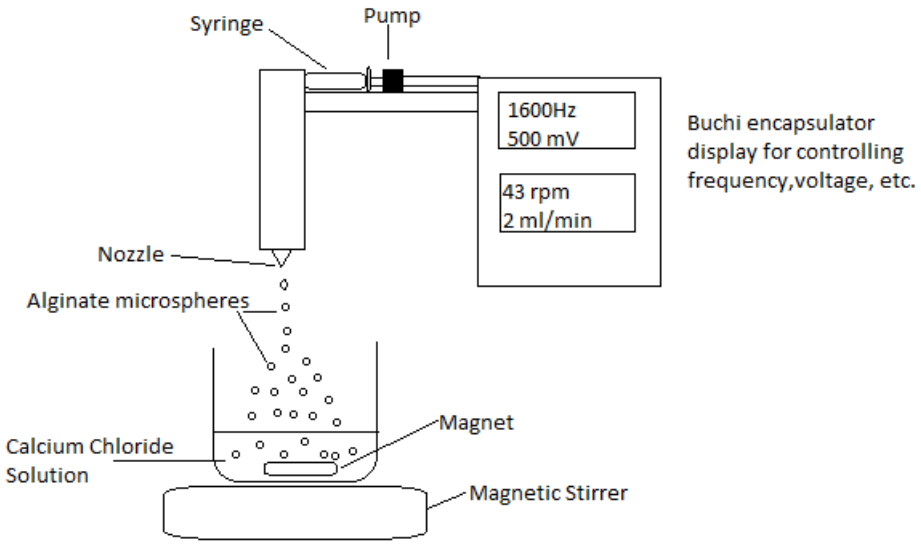

Figure 3.1. Schematic representation of calcium alginate microsphere production

Figure 3.2. Buchi Encapsulator B-395 Pro Apparatus

3.2 Drying of Empty Alginate Microspheres

The purpose of drying alginate microspheres was to be able to make them more usable for commercial uses as well. Drying them would increase their usability by increasing their

storage time and also making the storage process easier too. However, with the afore mentioned method of producing alginate microspheres there were some problems when dried. The microspheres, once dried, would burst and the water taken up during encapsulation by the microsphere would be completely let out, thus completely dehydrating the particle, making it lose its shape and sturdiness, and subsequently would result in the loss of the encapsulated substance when encapsulation was carried out. Thus, a new method had to be found for producing alginate microspheres that could hold their shape, not get dehydrated, and hold the material encapsulate within when dried. In literature it was observed that HPMC and Tween-85 was used, thus using an oil-in-water method for producing the microspheres. The reason as to why HPMC was used was because HPMC can be used as a stabilizing agent for gels, including Alginate gels, in addition to being used as thickening agents [76]. Additionally, HPMC has been shown to slow down drug release [77]. Therefore, HPMC was added into the alginate solution at a concentration ratio of 9:1 respectively. This concentration was obtained after various optimization tests for the Buchi Encapsulator of concentrations found from literature [77]. The cross-linker $CaCl_2$ solution had the surfactant Tween-85 added into it, so that the shear-force of the microspheres would not be able to affect the shape.

Briefly, to produce 50 ml of the alginate solution that will form the microspheres, 0.54 g of sodium alginate and 0.06 g of HPMC were added into 50 ml of distilled H_2O. This solution was then mixed thoroughly until a slightly viscous 1.2% alginate solution was obtained. To make the 100 ml 5% $CaCl_2$ cross-linker solution, 5 g of anhydrous $CaCl_2$ powder was added into 100 ml distilled water and 1 ml of Tween-85 was added as a surfactant. This solution was also mixed thoroughly via a magnetic stirrer. The alginate solution was then loaded into the syringe of the encapsulator and the machine was tuned to the following parameters: 1600 Hz frequency, 500 mV of electric voltage, and 2 ml/min flow rate, with a stirring speed of 43 rpm for the magnetic stirrer. The important factor here is that, due to the nozzle size being very small and thus prone to blockages, there should be no undissolved substances in the loaded alginate solution. Once the microsphere formation was complete and were collected into the beaker holding the cross-linker solution, they were left to further harden in the solution at a constant stirring for another hour. The microspheres were then washed with distilled H_20 three times and isopropyl alcohol twice for 8 minutes. The particles could then be dried in an oven.

3.3 SPION Synthesis

In literature there are many methods for the synthesis of superparamagnetic iron oxide nanoparticles for use in medical imaging techniques. These include emulsions (at the micro level), magnetized gels, synthesis via sono-chemistry, a hydrothermal approach utilizing a soft template, thermolysis and hydrolysis of precursors, synthesis by using electrospray, synthesis by flow injection (FIS) [68, 69]. In this case the classical co-precipitation method was utilized which was first coined be Rene Massart in his work related to developing magnetic Ferro fluids in basic and acidic media [70, 71]. This was the preferred method due to its ease in execution, cheapness, and the resulting synthesis of mostly uniform and small sized SPIONs. The most commonly used co-precipitation method is mixing iron salts (Fe^{2+} and Fe^{3+}) in 1:2 stoichiometric ratios respectively, so as to form a yellowish clear aqueous solution. Then, a basic solution is added dropwise slowly, to form a black precipitate which contains spherical magnetic iron oxide nanoparticles in uniform sizes. The whole process is carried out in an oxygen free environment. This is so that the production of ferric hydroxide is prevented in the solution, which can form due to too much oxidization. To adjust the size and shape of the nanoparticles, different amounts of ferrous or hydroxide ions could be added. In literature, it was also found that adding NaOH instead of NH_4OH dropwise resulted in smaller sized particles due to NaOH being a stronger base thus making the pH higher much faster [71]. Therefore, in this thesis, NaOH was also preferred. The following equation represents the general reaction: $Fe^{2+} + 2\ Fe^{3+} + 8OH^- \rightarrow Fe_3O_4 + 4H_2O$ [75].

The process was carried out thus: Into a round bottomed flask (Figure 11), 59.2 ml of dH_2O was added. 800 µl concentrated HCl (37%) was added and stirred vigorously via a magnetic stirrer. The flask was flushed with nitrogen gas for 15 minutes so as to remove any air and thus oxygen. The nitrogen gas tank was kept connected throughout the process. 5.2 g of $FeCl_3.6H_2O$ iron(III) salts and 2 g of $FeCl_2.4H_2O$ iron(II) salts were then added together at the same time into the flask so that a yellowish clear solution was formed. The temperature was then increased to 65ºC under vigorous stirring and N_2 gas atmosphere for 30 more minutes. During this time 1M 100 ml NaOH solution was prepared. After the 30 minutes from the previous step was completed, the NaOH solution was added dropwise into the solution using a needle. The solution immediately started turning into a black precipitate.

The development of a black precipitate showed that Super Paramagnetic Iron Oxide Nanoparticles (SPIONs) had been synthesized. After the 100 ml of NaOH was added, the solution was further stirred vigorously for 1 hour. The solution was then cooled to room temperature while still stirring for another 1 hour. Then, by using a strong magnet, the SPIONs were washed 4 times by decanting. The washed solution was then centrifuged at 12000 rpm for 15 minutes and poured into a petri dish and placed into a vacuum oven for 24 hours so that dried powder was obtained.

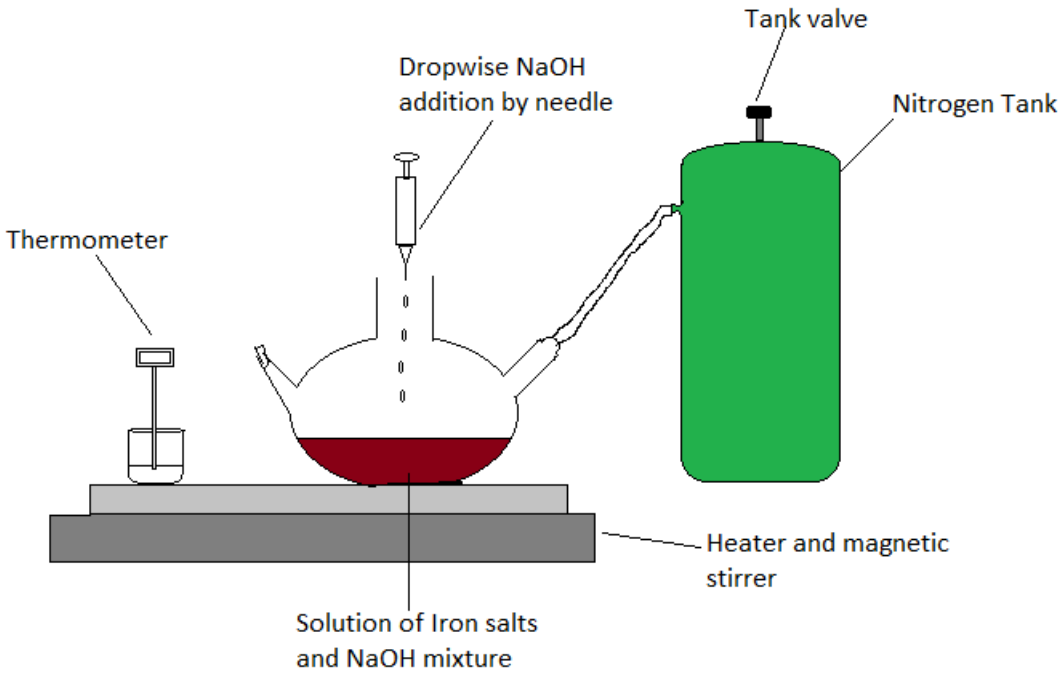

Figure 3.3. Schematic representation of the synthesis of superparamagnetic iron oxide nanoparticles

Figure 3.4. Apparatus for the synthesis of SPIONs

3.4 Characterization of SPIONs

The characterization of the super paramagnetic iron oxide nanoparticles consists of two different characterization areas. One of these encompassed the morphological characterization of the SPIONs, while the other encompassed the magnetization characteristics of the SPIONs. Both of these are explained in more detail below.

3.4.1 Morphological Characterization

To learn the shape and size of the SPIONs, a scanning electron microscope was used to visualize the particles at the nanoscale and measure the individual particle sizes and determine their shape and homogeneity. Additionally, before observing the shape and size of the nanoparticles, a Zeta Sizer (3000 HAS, Malvern, England) was used to determine the PDI, Zeta Potential, and the average size of the nanoparticles according to the maximum peak and the Zeta Size, where the Zeta Size was taken into account rather than the maximum peak as this value gives a more accurate representation of what the sizes of the nanoparticles are.

3.4.2 Magnetic Property Characterization

3.4.2.1 Electron Spin Resonance (ESR) Studies

Electron Spin Resonance (ESR) is an analysis technique for the magnetic properties of the molecules which have unpaired electrons. Due to the unpaired electrons of these molecules

they exhibit magnetic properties and by using this type of characterization technique it can be determined whether the analyzed materials have magnetic properties or not.

During the studies, prepared iron oxide nanoparticles and iron oxide nanoparticle loaded alginate microspheres were characterized with an ESR spectrometer (Bruker EMX 113 X-Band ESR, Germany). Optimum experimental conditions were given as follows.

Table 3.2. Experimental conditions for ESR studies

Central magnetic field	270.0 mT
Sweep range	500 mT
Microwave frequency	9.78 GHz
Microwave power	0,125 mW
Modulation frequency	100 kHz
Modulation amplitude	0.1 mT
Gain	$3.17x10^3$
Sweep time	83.89 s
Time constant	81.92 s
Temperature	Room Temperature

3.4.2.2 Determination of Magnetic Properties

Magnetic properties of prepared SPION nanoparticles and SPION nanoparticles loaded Alginate microspheres were evaluated with a vibrating sample magnetometer (Lake Shore, LDJ 9600 VSM, USA). These magnetic properties of the nanoparticles and microspheres in the magnetic field are expressed in units of electromagnetic force (emu), here in VSM measurements, magnetic field of constant frequency was applied on dried samples. During the experimentation, if the sample has magnetic properties it would act as a magnet due to the transient magnetic flow that creates a potential difference in the conductive rod.

Magnitude of potential difference giving out magnetization curve peaks were determined by a vibrating magnetometer.

3.4.2.3 Hyperthermia Studies

3.5 Synthesis of SPION Alginate Microspheres

To produce 25 ml of SPION Alginate microspheres, a 5 mg/ml concentration of SPIONs were used as this concentration was found to be ideal from both literature and various trials. 0.27g Alginate was added into 25 ml distilled H_2O. After the alginate was completely dissolved via vigorous stirring using a magnetic stirrer, 0.03g HPMC was added and the solution was continuously stirred until a smooth alginate HPMC solution was obtained. The resulting ratio of HPMC to alginate was 1:9. For the $CaCl_2$ solution, 5 g of $CaCl_2$ in anhydrous powder form was added to 100 ml of dH_2O and stirred vigorously until the solute was completely dissolved. 1 ml of Tween-85 was then added as a surfactant so that the shear force resulting from the free fall of the alginate micro droplets could be decreased as much as possible. This resulted in the shape of the microspheres being more homogenous and more spherical as a whole, as described previously. The dried SPIONs were then measured out and 125 mg were added into the alginate solution and sonicated for 40 minutes until the SPIONs were dispersed fully in the alginate solution [72, 73].

3.6 Synthesis of Sorafenib-SPION Alginate Microspheres

Due to sorafenib being insoluble in water, it first was needed to be dissolved in an organic solvent that would also not cause any damage to the cells in the body. It was found that methanol was an ideal solvent due to it being easily obtained and its cheapness. Additionally, it was found, in previous studies, that it was a good solvent for sorafenib to dissolve in [74]. Three different concentrations of sorafenib were tried and each concentration was separately tested in drug release and loading experiments which will be further explained in a later chapter [75].

To prepare the Sorafenib solution 200 mg of the Sorafenib Tosylate drug (one capsule) was placed into 20 ml of methanol which was then heated until a temperature of 65^{o}C was reached by placing the methanol into a 50 ml falcon which was then placed into a water bath that was heated using a heated magnetic stirrer apparatus which was previously used for the

synthesis of the iron oxide nanoparticles (Figure 3.4). Methanol was used to dissolve the drug instead of water as Sorafenib is insoluble in water. The resulting stock solution had a 10 mg/ml concentration of Sorafenib. After vigorously stirring the drug and methanol solution at 65ºC for a further 10 minutes, it was centrifuged for 5 minutes at 5000 rpm. The supernatant was then taken and was run through a 0.25 µl filter via a needle so that any other underlying substances that did not dissolve in the methanol and which were not gotten rid of by centrifuging, could be taken away and a pure Sorafenib methanol solution was left over for later use.

Two different methods were tested to find the best way for making Sorafenib SPION Alginate microspheres. Each method had 3 different formulations, each testing different concentrations of Sorafenib in the alginate solutions. The three concentrations of the Sorafenib drug that were tested were 1 mg/ml, 0.25 mg/ml, and 0.10 mg/ml. The first method consists of mixing the alginate, Sorafenib solution, and the iron oxide nanoparticle solution together with three different formulations each with one of the different Sorafenib concentrations mentioned previously. Each formulation was then mixed thoroughly by first using a vortex and then sonicating them for 45 minutes to 1 hour depending on their homogeneity, so that all the components were thoroughly dissolved and a final alginate concentration of 1.2% was obtained. Each formulation was then run separately through the encapsulator into the cross-linker solution to form Sorafenib-SPION-Alginate microspheres. The second method consisted of adding the drug into the cross-linker solution. The same 3 concentrations of the drug were prepared in the cross linker solution. These were 1) 1.5 g $CaCl_2$ + 90 ml dH_2O + 10 ml Sorafenib drug (10 mg/ml concentration), 2) 1.5 g $CaCl_2$ + 97.5 ml dH_2O + 2.5 ml Sorafenib drug (10 mg/ml concentration), and 3) 1.5 g $CaCl_2$ +99 ml dH_2O + 1 ml Sorafenib drug (10mg/ml concentration). 1.2% SPION alginate was prepared to be dropped from the Buchi Encapsulator into the cross linker solutions mentioned previously.

3.7 Characterization of Microspheres

For the characterization of microspheres, several apparatuses and methods were used. For the visualisation of the microspheres an optical microscope was used. Other characterization procedures included the calculation of the swelling ratio, the determination of the magnetic properties of empty alginate microspheres, SPIONs alone, and alginate microspheres +

SPIONs together to make a full comparison. Finally, drug loading and release analyses were carried out to determine how much the microspheres took in the drug sorafenib from the solution and if the release was constant and steady. These processes are explained in more detail below.

3.7.1 Optical Microscope

An Olympus Optical Microscope was used to visualise the Microspheres. Both the empty microspheres and the ones that had iron oxide nanoparticles were easily visualised and their photos were captured using a built in camera system.

3.7.2 Magnetic Property Characterizations of the Microspheres

As was described previously in the section describing the magnetic property characterization of the SPIONs, the same tests were carried out for the microspheres containing SPIONs and Sorafenib as well as empty alginate microspheres as a control. Both ESR and VSM tests were carried out as previously described.

3.7.3 Swelling Ratio Calculations

This process was carried out to determine the differences between alginate microspheres in solution, dried, and rehydrated with measurements taken at regular intervals of 0, 0.3, 2, and 4 hours. This was repeated for empty alginate microsphere and SPION-filled alginate microspheres so that a fully reliable analyses of how much the size of the microspheres changed according to the contents after drying and rehydration could be carried out.

The diameters of the microspheres were used to find the particle swelling percentage by subtracting the diameter of the microspheres at the time interval when the measurement was taken (where time=t, $[D_t]$) from the length measurement of the microsphere taken at the starting time when the water was first added (where t=0, $[D_0]$). The percentage was then calculated using the equation below:

$$\text{Swelling \%} = [(D_t - D_0)/D_0] \times 100$$

3.7.4 Sorafenib Drug Loading and Release

To test the ability of the microspheres in taking up the Sorafenib drug and then releasing it, drug loading and releasing tests were carried out. Once the Sorafenib SPION alginate microspheres were prepared (as described previously), the microspheres were tested for how

much of the Sorafenib drug was taken up by them, and how much of it was to be released once the microspheres entered the body and consequently the site of action. To do the drug release tests, an environment depicting the human body was simulated. This was carried out by preparing a water bath of approximately 37ºC (representing the average human body temperature) into which the alginate microspheres, contained in 50 ml falcons containing PBS, were placed in. The water bath was then left to gently shake the microsphere solutions for 72 hours (3 days). Absorbance measurements were taken regularly starting with every 15 minutes and gradually increasing the time intervals between absorbance measurements until the last measurement was taken 50 hours after the previous measurement.

Before getting the solutions ready for drug release testing, the Sorafenib encapsulation ratio had to be calculated to determine the amount of drug loaded into the microspheres. The first step for this procedure was to get the newly produced SPION Sorafenib Alginate microspheres, found in 50 ml falcons containing Calcium chloride solution, and centrifuging them at 3500 rpm for 3 minutes. The second step was to take approximately 1 ml from the supernatants of all of the falcon tubes and place them in labelled Eppendorf tubes. The absorbance of these supernatants were then measured at an absorbance wavelength of 263 nm and 226 nm using a UV Spectrophotometer. Finally, the rest of the supernatants in the falcons, were poured out leaving only the microspheres at the bottom of the falcons as a pellet to be later used for drug release tests.

To begin the drug release tests, the first step was to prepare the PBS solution which was to be used as the medium for measuring the drug release. To do this, a PBS tablet was dissolved in 100 ml of distilled water. Two different drug release tests were carried out. Each test had 4 different concentrations of Sorafenib in the microspheres with two 0.25 mg/ml Sorafenib with no SPIONs. These were: 0.25 mg/ml without SPIONs, 0.1 mg/ml, 0.25 mg/ml, and 1.0 mg/ml. One test was carried out in 10 ml of PBS solution and the other was carried out in 20 ml of PBS solution. Therefore, there were a total of 8 samples which were tested for drug release. All the falcons were placed in the water bath previously mentioned and the test was started. As stated in the beginning of this section, the water bath containing the falcons was at 37ºC and rocked constantly with measurements taken at specific times. Additionally, before the absorbance measurements were taken, the samples obtained at each time interval were mixed with 65ºC methanol at a 7:3 (sample to methanol respectively) ratio.

3.8. Preparation of the L292 cell lines

To be able to test the effect that the Sorafenib-SPION Alginate microspheres would have on the healthy cells surrounding the cancer cells, healthy Mouse Fibroblast cell (L292) were used for the cytotoxicity and biocompatibility tests by transfecting the microspheres on the L292 cells with different test groups that had different concentrations of Sorafenib in the microspheres.

To grow the L292 cell line healthily without the growth of bacteria or other impurities, the medium used had to be prepared accordingly. Therefore, the DMEM medium that was to be used for this purpose had 100 µg/ml of Streptomycin added in addition to 100 U/ml of Penicillin and 2 mM of L-Glutamic acid. This medium composition was then placed in to a cell growing flask in addition with the L292 cells and incubated in an incubator with a temperature of 37^{o}C and 5% CO_2 environmental conditions for 24 hours. Every 24-hour period, the flask was checked under the microscope to see if any bacterial or fungal growth was observed in the medium. Once the cells reached a confluence of approximately 80 to 90%, a one quarter (1/4) passage was carried out where the cells were relocated onto a new flask. Once the cells increased in numbers once more, the enzyme trypsin was placed on to the cell culture so that the cells could be released from the bottom of the flask.

Table 3.3. The environment in which the L292 cell lines grow in

Cell type	Mouse Fibroblast Cell Line (L292)
Petri dish	75 cm^2 polystyrene flask (T75), appropriate for cells attaching to surface
Cultural Property	Adherent
Features of culture	Monolayer
Routine subculture	1⁄4
Total volume	5 mL

pH	7.2-7.5
Temperature	37±0.5ºC
Incubation medium	5 % CO_2, humid, in an incubator

3.9 Cell Interaction and MTT Tests of Sorafenib-SPION Alginate Microspheres

To investigate the effect of the Sorafenib-SPION Alginate microspheres on healthy cells that are found in the surrounding areas of the tumour cells, MTT tests were carried out on L292 (mouse fibroblast cells). To carry out the MTT test, the microspheres were first prepared as previously stated and were therefore ready for transfection. Three different concentrations of the Sorafenib drug were used to prepare three different MTT tests. These concentrations were 0.1 mg/ml, 0.25 mg/ml, and 1.0 mg/ml. After the microspheres were prepared they were freeze died via lyophilisation. They were then diluted and rehydrated using the medium DMEM (Dulbecco's Modified Eagle Medium). The L929 cells were placed in to plates containing 96 wells ($5x10^3$ cells in each well) and left to incubate overnight so that the cells could attach themselves on the bottom of the wells via adhesion. The microsphere groups previously mentioned with different concentrations of Sorafenib were freshly prepared and diluted with the medium with a positive control medium group containing no microspheres. For microsphere transfections, firstly 50 µl of solution with the relevant microsphere was added onto the cells. After an incubation time of 1 hour, 50 µl DMEM that had no serum was added so that a final concentration of 100 µl was obtained in each well. The L292 plates were then left to incubate for first 24 hours and a further 48 hours for analysing cell cytotoxicity.

3.9.1. Determination of L292 cells cytotoxicity

To be able to investigate the toxicity of the SPION Sorafenib Alginate microspheres with different Sorafenib concentrations on L292 cells, a colorimetric MTT test was carried out.

In a colorimetric MTT test yellow MTT is placed in to the wells as, when it comes into contact with an enzyme known as mitochondrial dehydrogenase found in cells, it becomes reduced and crystals known as formazan crystals of MTT begin to appear resulting in the

formation of a purple colour. This happens due to the dye diffusing through the membranes of dead cells only. Once the plates were incubated for 24 and 48 hours (as mentioned previously), the previously placed media was removed and 90 µl of new DMEM media in addition to 10 µl MTT agent (concentration of 5 mg/ml that was diluted using PBS) was added on to the cells. A further incubation of the plates was carried out in an incubator that had atmospheric properties of 37ºC and 5% CO_2 in a humid environment. Before incubation, the plates were covered in aluminium foil. After incubation, acidic isopropanol (isopropanol containing 0.04 M HCl) of an amount of 100 µl was put in place of the MTT solution which was removed. The aluminium foil left on top of the plates which were left to incubate a further 30 minutes in room temperature so that the formazyl crystals could fully be dissolved via the isopropanol. Next, the MTT solution was replaced with 100 µl of acidic isopropanol (0,04 M HCl included isopropanol). For processing the ELISA plate colour changes an ELISA microplate reader was used to measure the absorbance of the plates using a wavelength of 570 nm for the measurements. 8 replicates of the MTT test were carried out for each group tested and for the control group. It is expected that the lesser the concentration of Sorafenib in the microspheres the higher the cell viability of the L292 cells will be.

4. EXPERIMENTAL RESULTS AND DISCUSSION

4.1 Optimization of Empty Calcium Alginate Microspheres

The 0.1%, 0.5% and 1% were not carried on with as these concentrations were too less to result in microsphere production. When the microspheres landed into the $CaCl_2$ solution, very little crosslinking occurred. The concentrations that were kept in the study were as follows: 1.5%, 5%, and 10% $CaCl_2$ solutions.

The results below show the microspheres obtained from these optimization tests.

Graph 4.1. Mean length of microspheres for a 1.2% Alginate Solution and 1.5% $CaCl_2$ cross linker solution

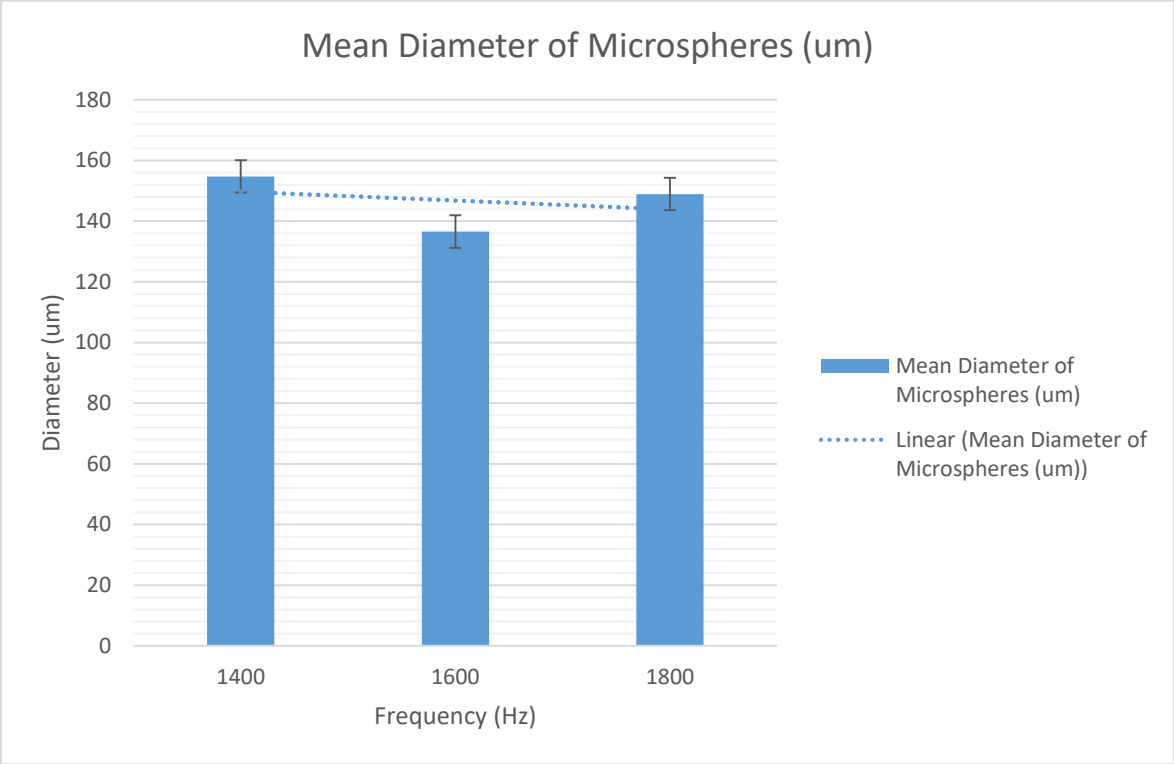

Table 4.1. Mean length of microspheres for a 1.2% Alginate Solution and 1.5% CaCl2 cross-linker solution and photos of the microspheres taken with a microscopic camera.

Frequency (Hz)	Mean Diameter of		Standard Deviation

	Microspheres (um)		
1400	154.8	See Figure 4.1 A	33.97
1600	136.6	See Figure 4.1 B	17.03
1800	149.0	See Figure 4.1 C	9.36

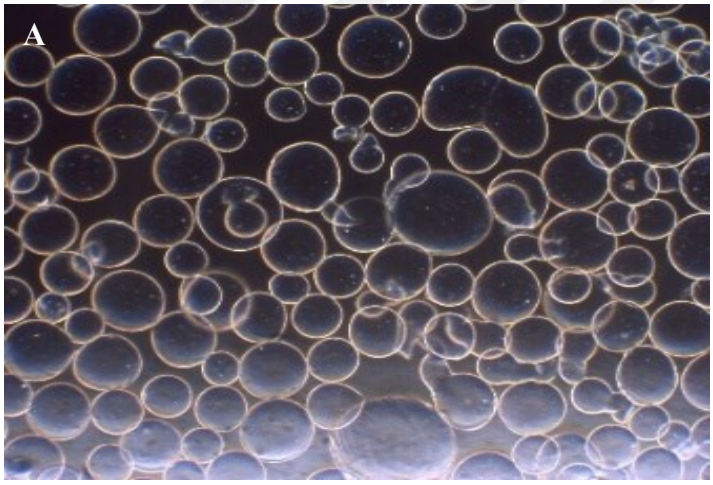

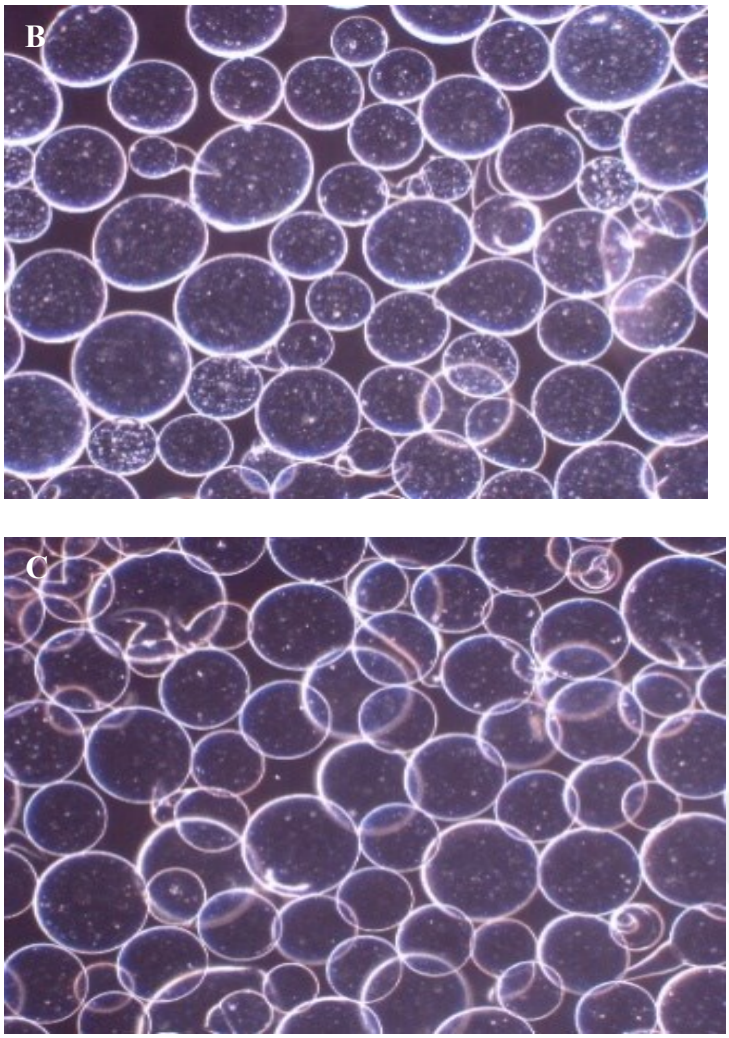

Figure 4.1. Images of the empty alginate microspheres produced at CaCl2 concentration of 1.5% and A) 1400 Hz, B) 1600 Hz, and C) 1800 Hz

For the 1.5% $CaCl_2$ crosslinking solution, it was found that 1600 Hz resulted in the smallest and most homogenous microspheres. As can be observed in the graph and table above, the mean length of the microspheres was measured to be 136.58 μm for the 1600 Hz frequency with the 80 μm nozzle. The lengths were measured by photographing the microspheres observed via a light microscope, at a 4x magnification, and converting the photograph into a file that is visible by the j image programme, from which 90 length measurements were taken of the microspheres obtained from each frequency. The average was then calculated and a table was constructed (Table 1) and subsequently a graph (Graph 1). Interestingly, it can be observed that even though the smallest microspheres were obtained from the 1600 Hz frequency, the lowest amount of standard deviation of the microsphere lengths existed for the 1800 Hz frequency.

Graph 4.2. Mean length of microspheres for a 1.2% Alginate Solution and 5% $CaCl_2$ cross-linker solution

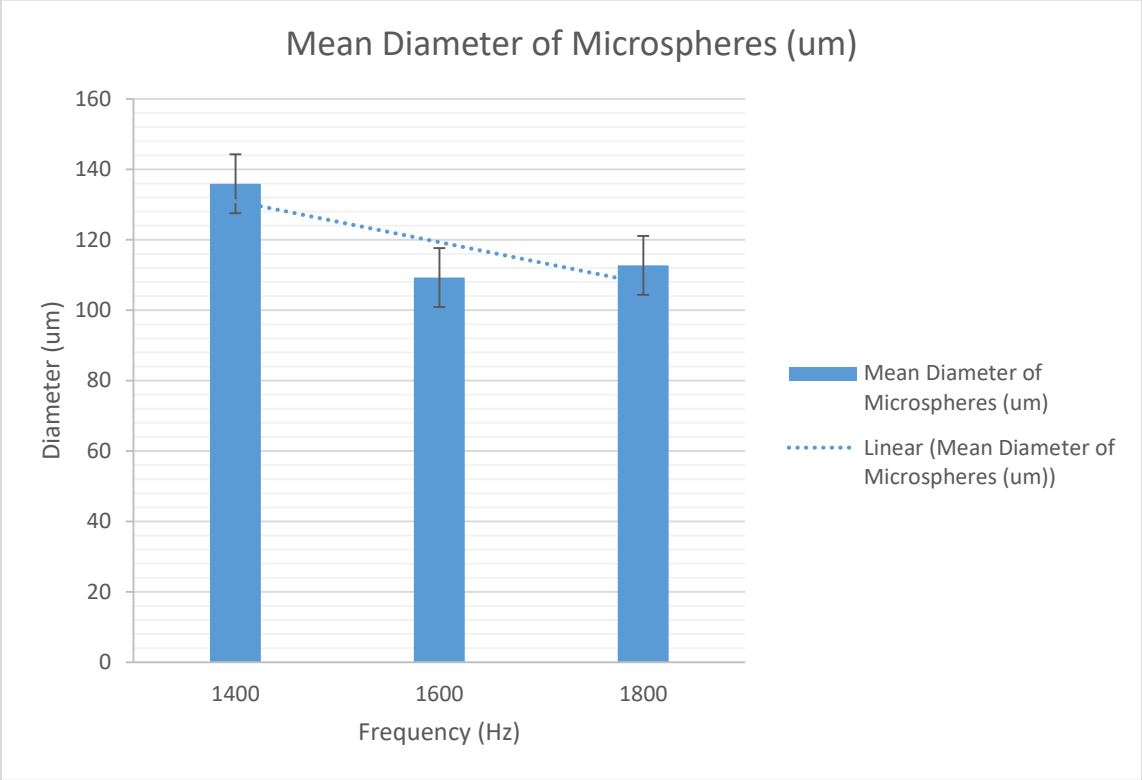

Table 4.2. Mean length of microspheres for a 1.2% Alginate Solution and 5% CaCl2 cross-linker solution and photos of the microspheres taken with a microscopic camera.

Frequency (Hz)	Mean Diameter of Microspheres (um)		Standard Deviation
1400	135.9	See Figure 4.2 A	18.49

1600	109.3	See Figure 4.2 B	5.08
1800	112.7	See Figure 4.2.3	3.27

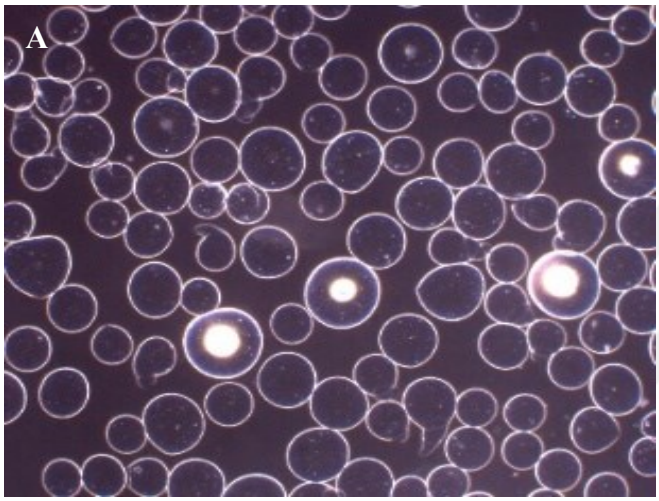

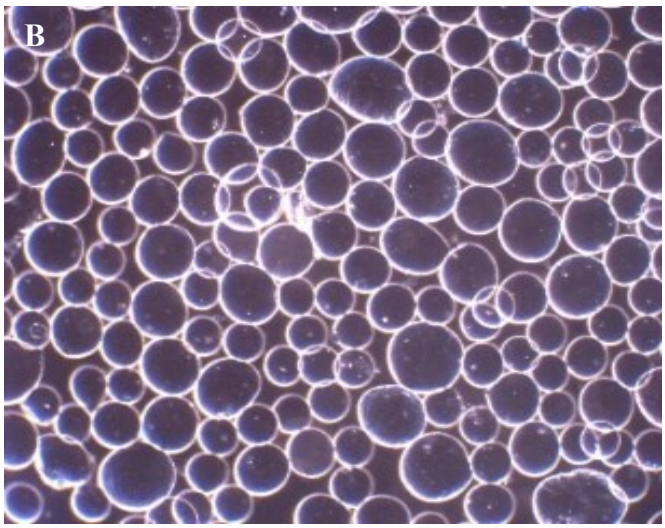

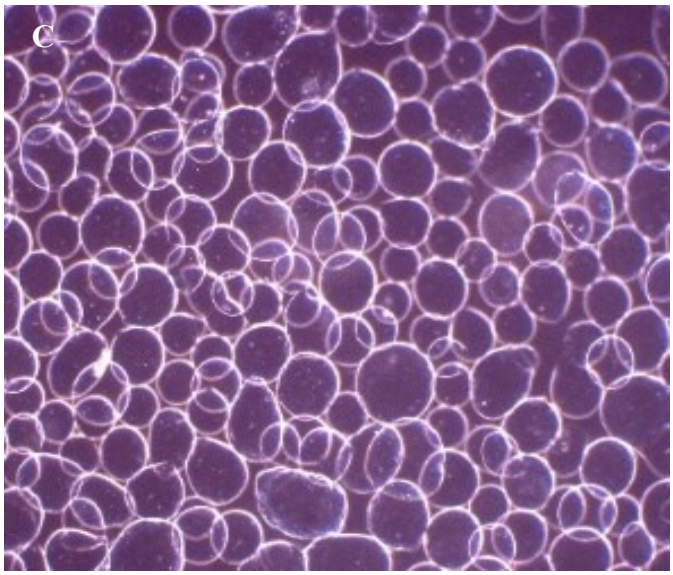

Figure 4.2. Images of the empty alginate microspheres produced at CaCl2 concentration of 5% and A) 1400 Hz, B) 1600 Hz, and C) 1800 Hz

For the 5% $CaCl_2$ solution it can be observed that the smallest mean length among the tested frequencies was shown by the 1600 Hz frequency, even though the standard deviation was slightly higher than that seen for the microspheres produced with the 1800 Hz frequency, the length of the microspheres remains significantly smaller. Therefore, it can be deduced from these results that the 1600 Hz was the best frequency for the 5% cross-linker solution. The largest mean length was observed in the microspheres produced by the 1400 Hz frequency.

Graph 4.3. Mean length of microspheres for a 1.2% Alginate Solution and 10% $CaCl_2$ cross-linker solution

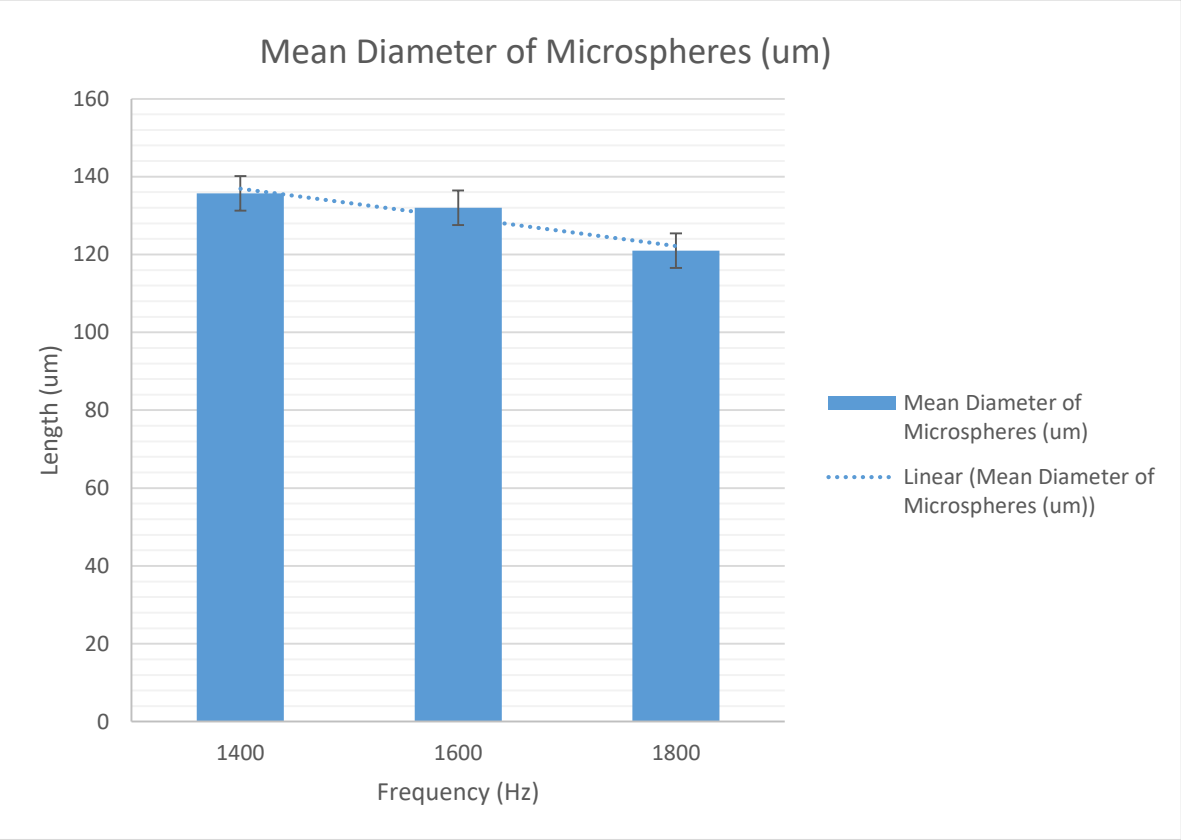

Table 4.3. Mean length of microspheres for a 1.2% Alginate Solution and 10% CaCl2 cross-linker solution and photos of the microspheres taken with a microscopic camera.

Frquency (Hz)	Mean Diameter of Microspheres (um)		Standard Deviation
1400	135.7	See Figure 4.3.1	11.46
1600	132	See Figure 4.3.2	5.98

1800	121	See Figure 4.3.3	11.71

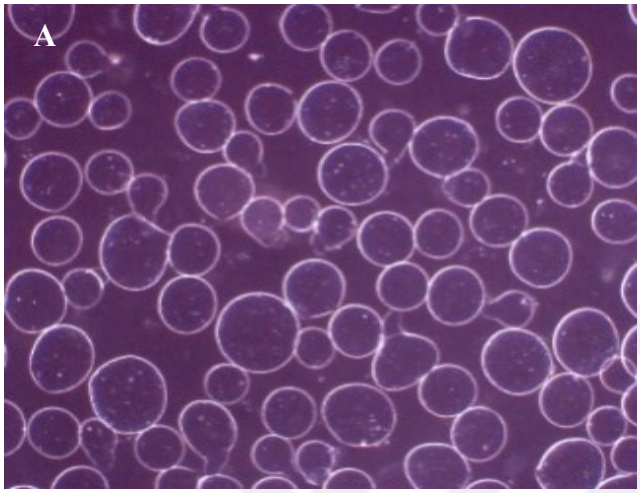

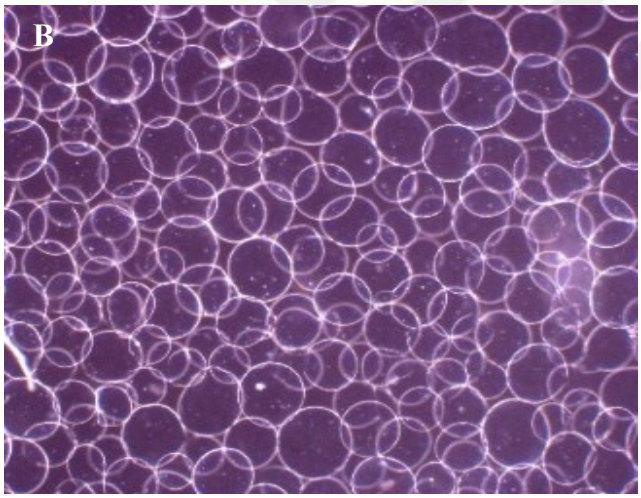

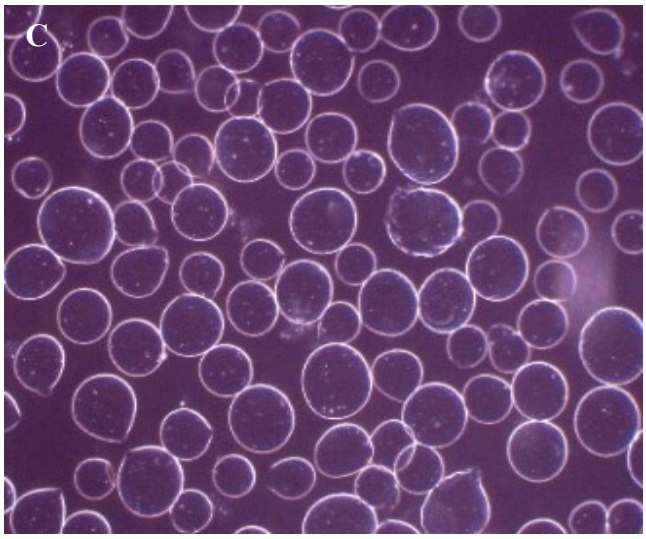

Figure 4.3. Images of the empty alginate microspheres produced at CaCl2 concentration of 10% and A) 1400 Hz, B) 1600 Hz, and C) 1800 Hz

For the 10% $CaCl_2$ crosslinking solution, even though the smallest size microspheres were seen when a frequency of 1800 Hz was applied, the homogeneity of the microspheres were not as good as when the 1600 Hz frequency was applied. This can also be seen from the standard deviation values which were 9.10 and 13.32 for the 1600 Hz and 1800 Hz frequencies respectively, thus showing a greater similarity in sizes for the applied frequency of 1600 Hz. As can be observed in the graph and table above, the mean length of the microspheres was measured to be 123 μm for the 1600 Hz frequency with the 80 μm nozzle. As mentioned previously, the lengths were measured by photographing the microspheres observed via a light microscope, at a 4x magnification, and converting the photograph into a file that is visible by the j image programme, from which 90 length measurements were taken of the microspheres obtained from each frequency. The average was then calculated and a table was constructed (Table 4.3) and subsequently a graph (Graph 4.3).

4.2 Drying of Alginate Microspheres

Drying the alginate microspheres have various advantages, including being able to store them easily without disrupting their shapes and contents. However, when empty alginate microspheres were dried after leaving them to harden further in the calcium chloride cross linker solution, they were found to have burst, shrunk and completely lost their shapes as can be seen in figure 4.1.A. Thus, a new formulation was tried where HPMC was added to the alginate solution so as to result in a 1:9 HPMC to alginate ratio in the final solution.

Additionally, 1 ml of Tween-85 was added in to the 100 ml cross linker solution so as to decrease the shear force occurring from the free fall of the microspheres. After drying these microspheres, it was found that they kept their shape completely, didn't decrease as much in size, and didn't burst. Dried microspheres with the new formulation can be seen in figure 4.4.B.

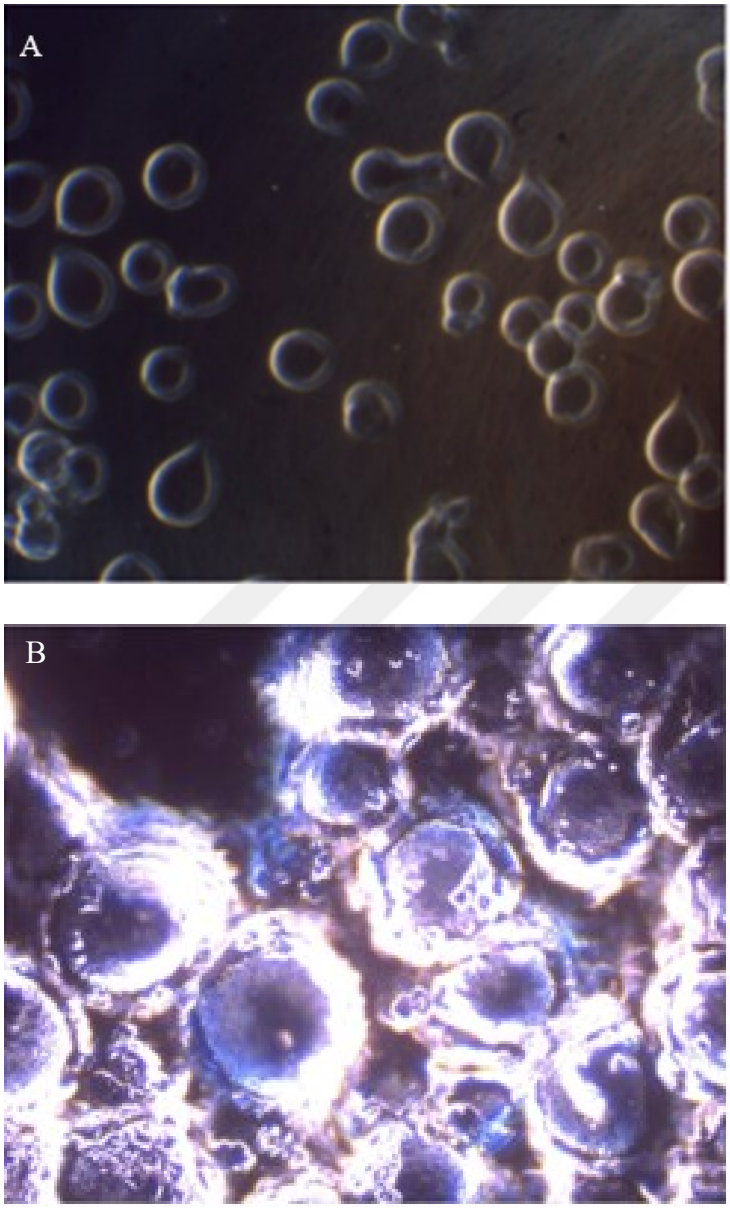

Figure 4.4. Light microscope images of dried empty alginate microspheres (A) before the addition of HPMC and Tween-85, and (B) after the addition of HPMC and Tween-85

4.2.1 Swelling Ratio results of the Microspheres

As can be observed from Graph 4.4., both the SPION filled alginate microspheres and the empty alginate spheres show an increase in volume with increasing time. This can be attributed to the microspheres swelling and, due to the levelling off at approximately 80% for the empty alginate microspheres, reaching a relatively initial volume to before drying. It can also be observed that there is a significant difference between the volumes of the SPION filled alginate microspheres to the empty ones with respect to swelling percentages. This could be attributed to the SPIONs found in the alginate microspheres as they prevent the alginate molecules from being too tightly packed together. This results in more water being taken in when rehydrated once dried. The opposite can be seen in empty alginate microspheres which showed less swelling as they could not take in as much water as those with SPIONs encapsulated within.

Graph 4.4. Representation of SPION Alginate and Empty Alginate microsphere swelling percentages.

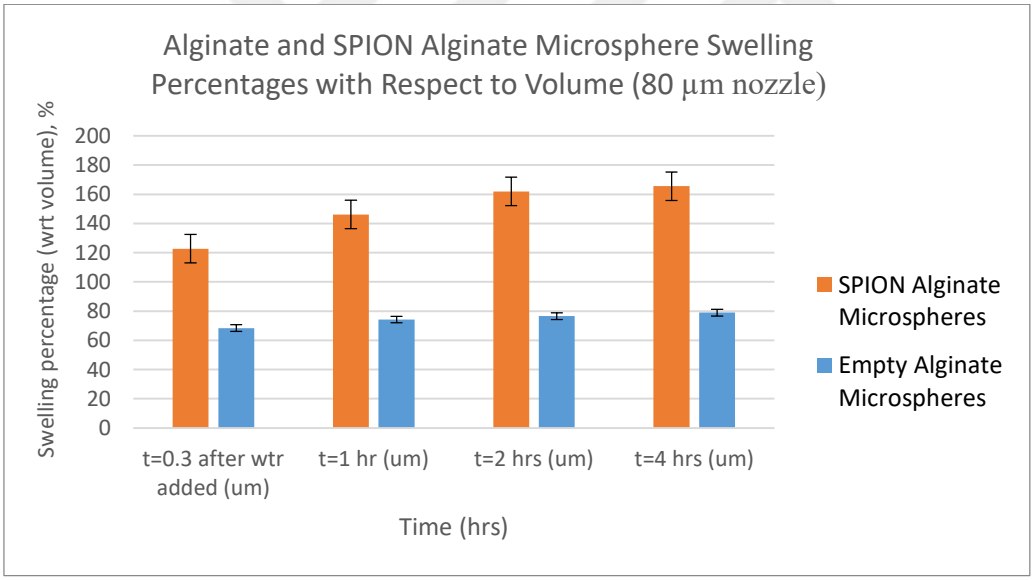

4.3 Synthesis and Characterization of SPIONs and SPIONs Encapsulated by Alginate Microspheres

4.3.1 Morphological Characterization of SPIONs

4.3.1.1 Zeta Potential and Size Distributions of SPIONs

From the graph below, it can be observed that the size distribution of the SPIONs were approximately 60.93 nm with a PDI of 0.267 showing that there was a general homogeneity

in the sizes of the nanoparticles. The zeta potential of the SPIONs were found to be -14.5 mV. The effect of surface charge on the binding of SPIONs were tested by hemo-dialysing the SPION solution in a HCl bath where 800 µl of pure 37% HCl was added in to 600 ml of distilled water. However, no significant difference was observed between positively charged SPIONs and negatively SPIONs in their encapsulation by the alginate microspheres. In fact, hemo-dialysing, resulted in greater aggregation of SPIONs which was a factor that was disadvantageous. Therefore, the negatively charged, non-dialysed formulation of SPIONs were used in further experiments.

Graph 4.5. Size distribution and PDI of the super paramagnetic iron oxide nanoparticles measured by the zeta sizer

			Size (d.nm...	% Intensity:	St Dev (d.n...
Z-Average (d.nm):	60,93	Peak 1:	81,92	97,9	51,41
PdI:	0,267	Peak 2:	4451	2,1	901,6
Intercept:	0,832	Peak 3:	0,000	0,0	0,000
Result quality	Good				

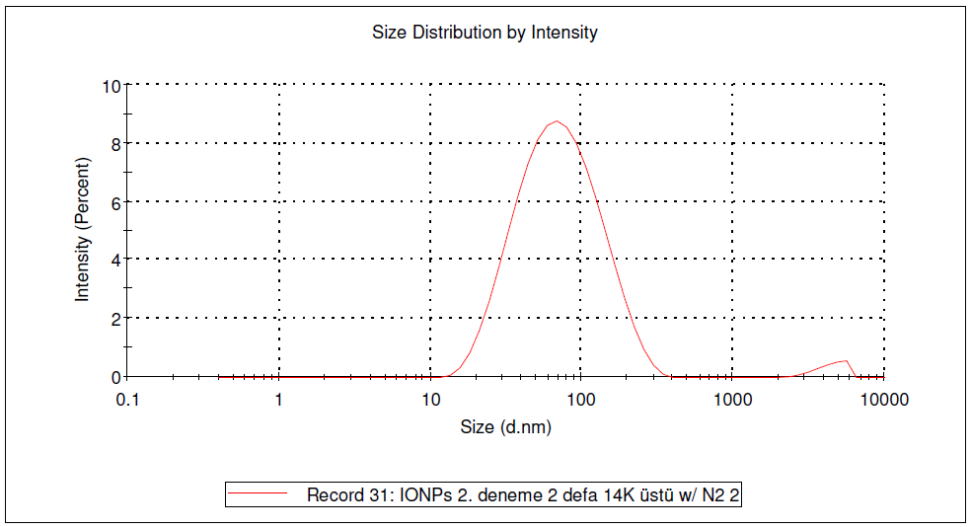

4.3.1.2 SEM Images of SPIONs

From the scanning electron microscope images, it can be observed that the SPIONs were much smaller than first measure by the zeta sizer which showed a size distribution of approximately 60 nm. However, it can be observed the images below that this size was much smaller, with the nanoparticles showing sizes of approximately 20 nm. It can also be observed that the nanoparticles are very much homogenous in size and morphology, with

each particle showing distinctly spherical shapes. This shows that the formulation resulted in relatively stable, homogenously sized nanoparticles.

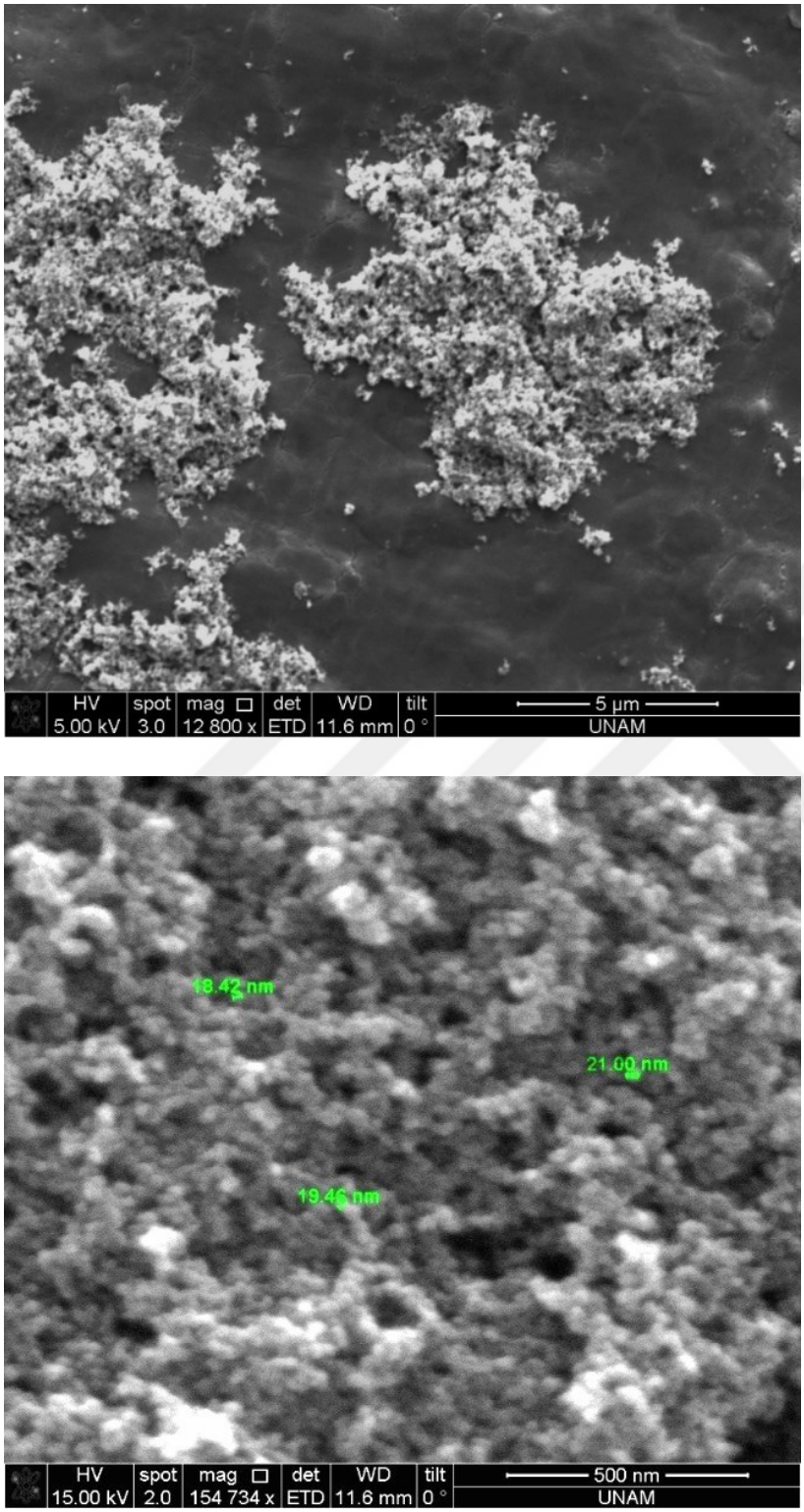

Figure 4.5. SEM representations for the super paramagnetic iron oxide nanoparticles (SPIONs)

4.3.2 Magnetic Property Characterizations

4.3.2.1 Electron Spin Resonance (ESR) Studies

ESR spectrums of SPION nanoparticles and Alginate/SPION Microspheres were given in Figure (A) and (B) respectively. When we compare the ESR signal strengths of the samples, this value is around 300.000 k.b. for SPION nanoparticles while its around 100.000 k.b. for Alginate/SPION microcapsules.

Graph 4.6. ESR Spectrums of SPION Nanoparticles (A) and Alginate/SPION Microspheres (B)

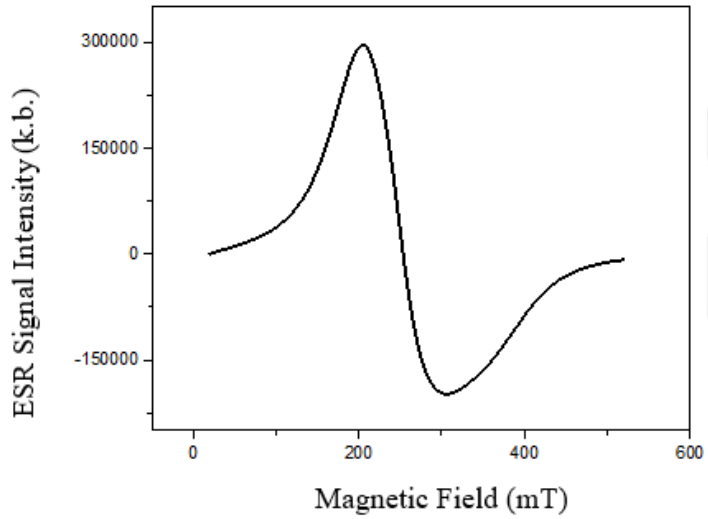

(A)

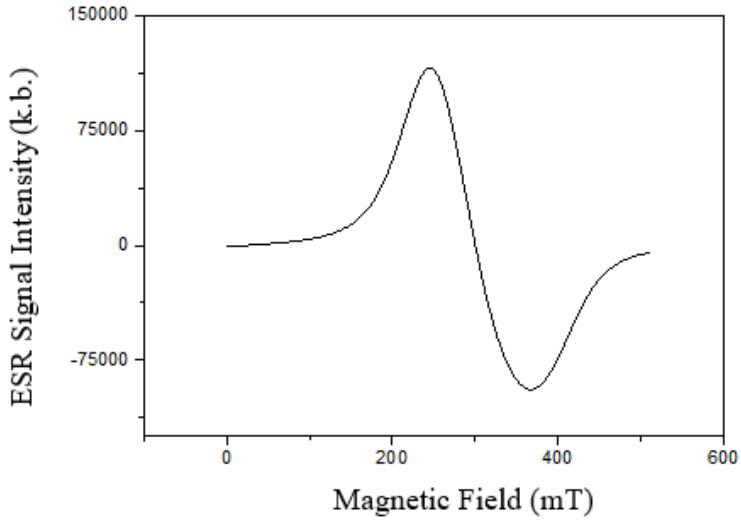

(B)

Therefore, we can tell that the magnetic field strength of the SPION nanoparticles were three times higher than Alginate/SPION microspheres according to these results. The spectral parameters for the SPION nanoparticles and SPION nanoparticles loaded Alginate microspheres were given in Table 4.4. As seen in this Table the g value for SPION nanoparticles was found as 2,759 while it was found 2,240 for SPION loaded Alginate nanoparticles as expected. This is because of the superparamagnetic structure of the SPION nanoparticles and shield effect of the polymeric (or diamagnetic) nature of the Alginate in the case of SPION nanoparticles loaded Alginate microspheres. Another important output was observed as saturation values of the SPION nanoparticles and SPION nanoparticles loaded Alginate microspheres as 3400 and 3800 mT respectively as expected. Because it's more difficult to agitate the SPION nanoparticles when they were loaded into the Alginate polymer as in the case of microsphere form due the diamagnetic nature of the alginate polymer.

Table 4.4. Spectral parameters for the SPION and Alginate/SPION samples

Sample	Line length from Peak to Peak ΔH_{pp} (mT)	Spectroscopic Splitting Factor g value	Magnetic Field of the Spectrum (mT)
SPION	100	2,759	340
Alginate/SPION	120	2,240	380

4.3.2.2 Magnetization Changing with Different Magnetic Fields

As can be seen in Figure 4.7, maximum magnetic quality (i.e. around 70 emu/g materials) was achieved in the case of SPION nanoparticles while this quality value was down to 4.0 emu/g SPION nanoparticles and 2.5 emu/g Alginate/SPION microspheres respectively. These behaviours can be explained with bare structure of SPION and alginate covering the SPION nanoparticles in microspheres form. On the other hand, the lowest magnetic quality value was obtained in the case of washed Alginate/SPION microspheres, this is most probably due to the released SPION nanoparticles which surrounded by microspheres during the washing procedure. As an another result around 10 kOe magnetic field was found to be

sufficient to excite almost all of the dipole moments of 1.0 g any nanoparticles or microspheres.

Graph 4.7. Magnetic properties of the SPION nanoparticles and SPION loaded Alginate microspheres

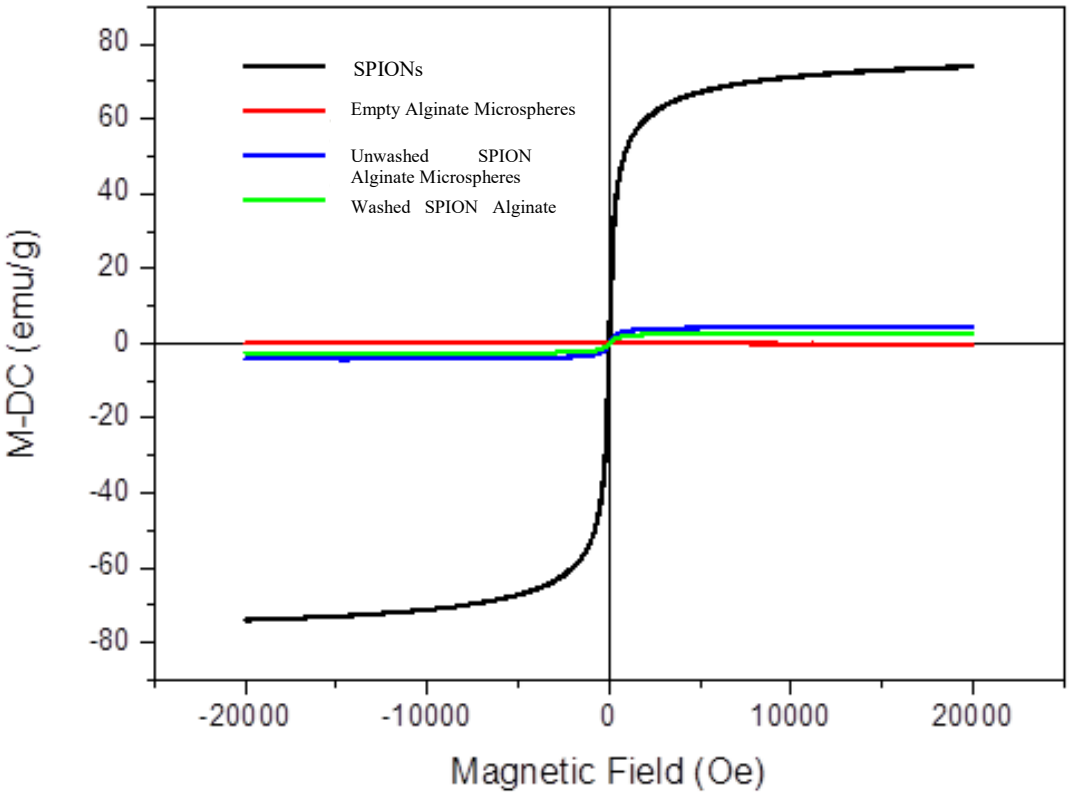

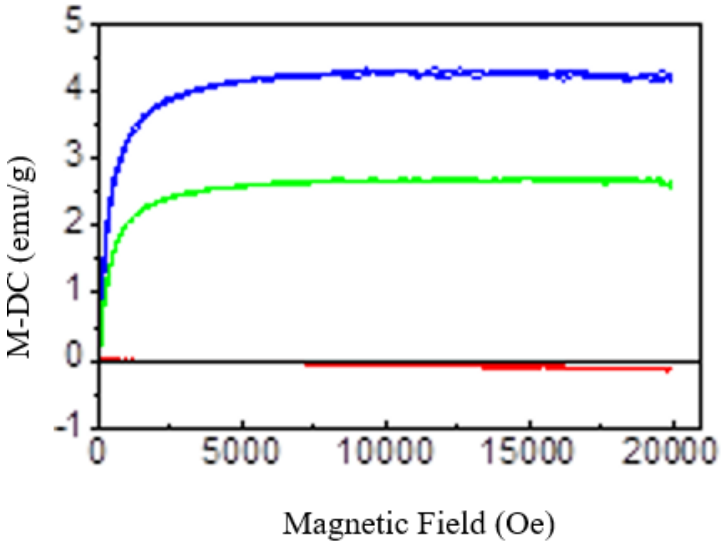

4.3. Hyperthermia Studies (Heating Performance of the Samples under AC Magnetic Fields)

As seen from Graph 4.8., iron oxide and both its washed and unwashed samples can heat the environment and can be used in hyperthermia area, which was one of the scope of this study. Besides the washed and unwashed samples showed relatively low changes in temperatures depending on storing time when their results were compared with the results of iron oxide samples. On the other hand, alginate sample did not exhibit the sample property, once more confirming the results recorded with ESR and VSM studies held for alginate samples.

Graph 4.8. Representation of the results obtained for the heating performance studies carried out on sample

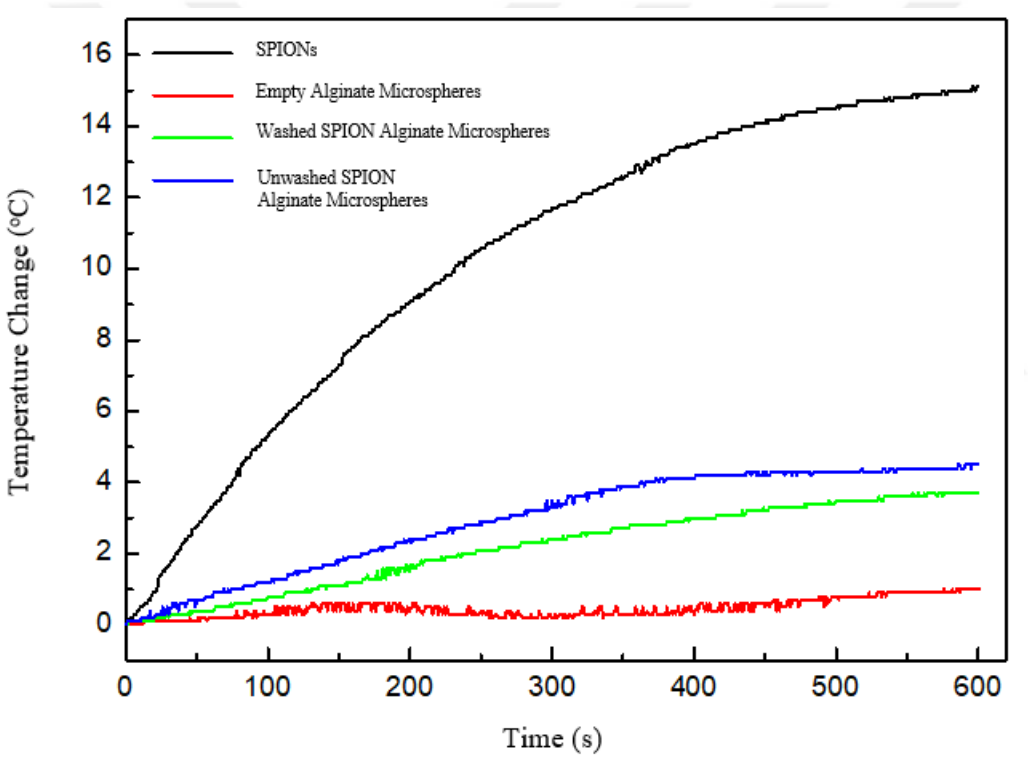

Table 4.5. Calculated SAR Values

Sample	SAR (J/gs)
SPIONs	99,3
Unwashed Alginate SPION microspheres	22,7
Washed Alginate SPION microspheres	16,5

4.4 Drug Loading and Release Test

As described previously, drug loading and release tests were carried out over a significant period of time (10 hours) and, as can be observed from graph 4.9., after a steep initial increase in drug release, this increase levelled off until no increase was observed.

Graph 4.9. Representation of drug release results measured throughout 10 hours

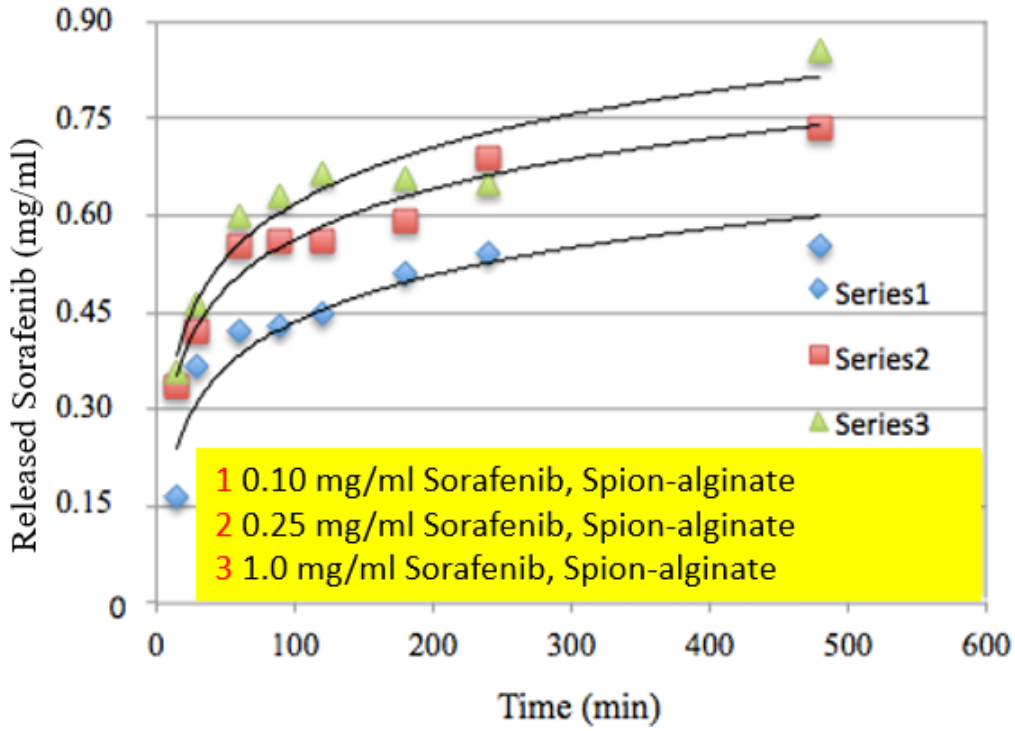

4.5 Cytotoxicity Tests

The cytotoxic effect of Sorafenib loaded Alginate-SPION microspheres against L929 mouse fibroblast cell line was studied using a MTT test. The results show low cytotoxicity for Alginate-SPION microspheres in L929 cells for 10, 100, and 500 µg/ml concentration. In the tests carried out with 10 µg microspheres (Graph 4.10.1.), the cell viability values of the SPION-Alginate microspheres containing different concentrations of Sorafenib were found to be relatively close to each other. Due to microspheres that do not contain SPIONs encapsulating a larger amount of Sorafenib, their cell viability value was found to be around 94%. When the particle amount was increased to 100 µg/ml, it was observed that the microspheres containing 1.0 and 2.5 mg/ml concentrations of Sorafenib had the same values as those that did not contain none of the drug and that no cytotoxic effect was observed (Graph 4.10.2.). While the microspheres containing a Sorafenib concentration of 10mg/ml resulted in 85% cell viability due to the high drug concentration. When the amount of microspheres was increased to 500 µg/ml, it was observed that the microspheres containing a concentration of 1.0 mg/ml Sorafenib had the same cell viability value with those that contained no drug and that as microsphere amount was increased, cell viability decreased due to the increase in drug amount (Graph 4.10.3). Also, comparing the cytotoxicity for Alginate-SPION and Alginate microspheres for 2,5 mg/mL Sorafenib in all microsphere concentrations, the Alginate-SPION microspheres were found to be more biocompatible due to their low drug encapsulation property.

Graph 4.10.1. Cell cytotoxicity test carried out with a concentration of 10 µg/ml microspheres

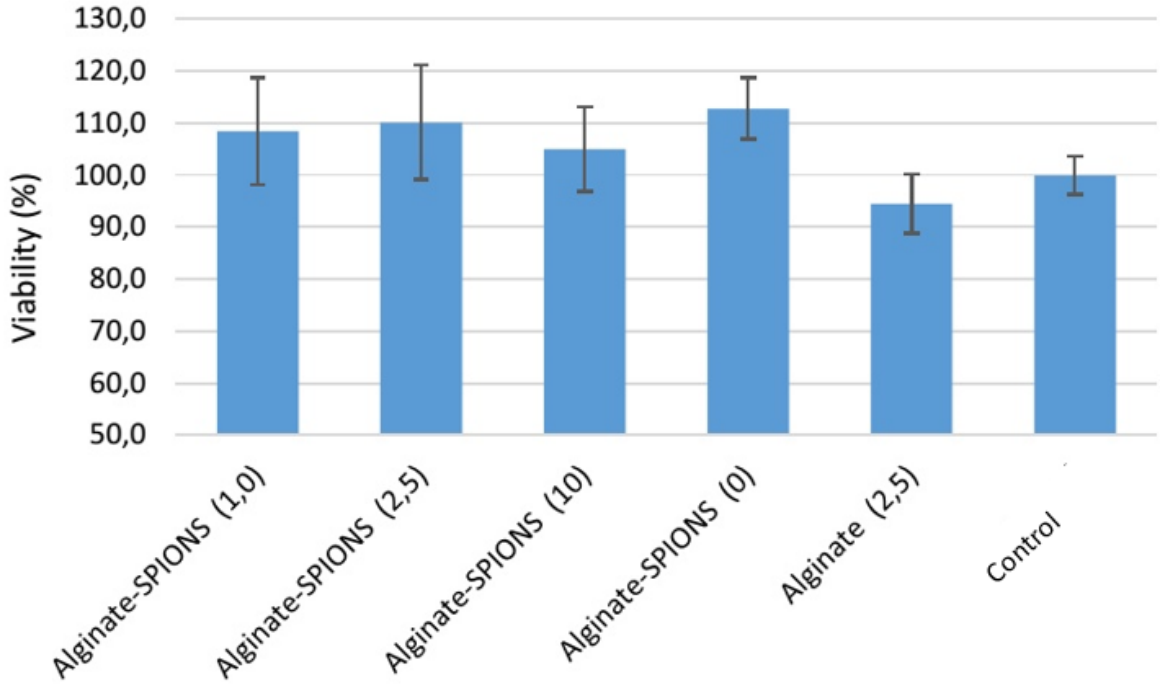

Graph 4.10.2. Cell cytotoxicity test carried out with a concentration of 100 µg/ml microspheres

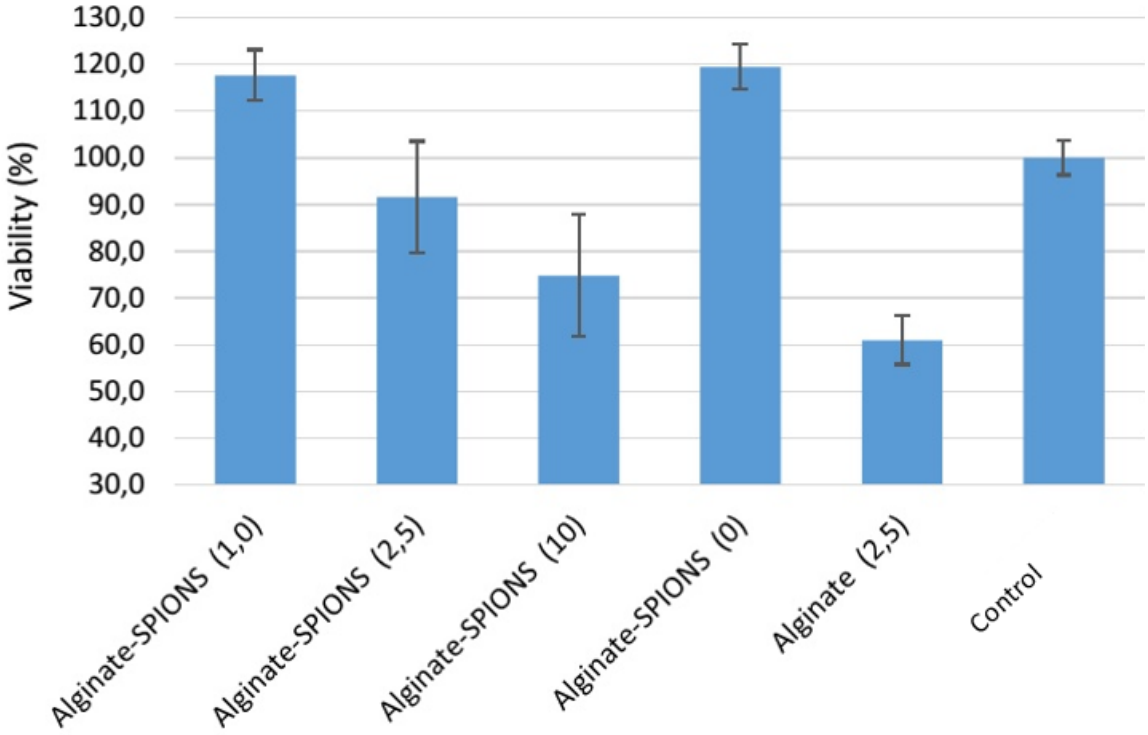

Graph 4.10.3. Cell cytotoxicity test carried out with a concentration of 500 µg/ml microspheres

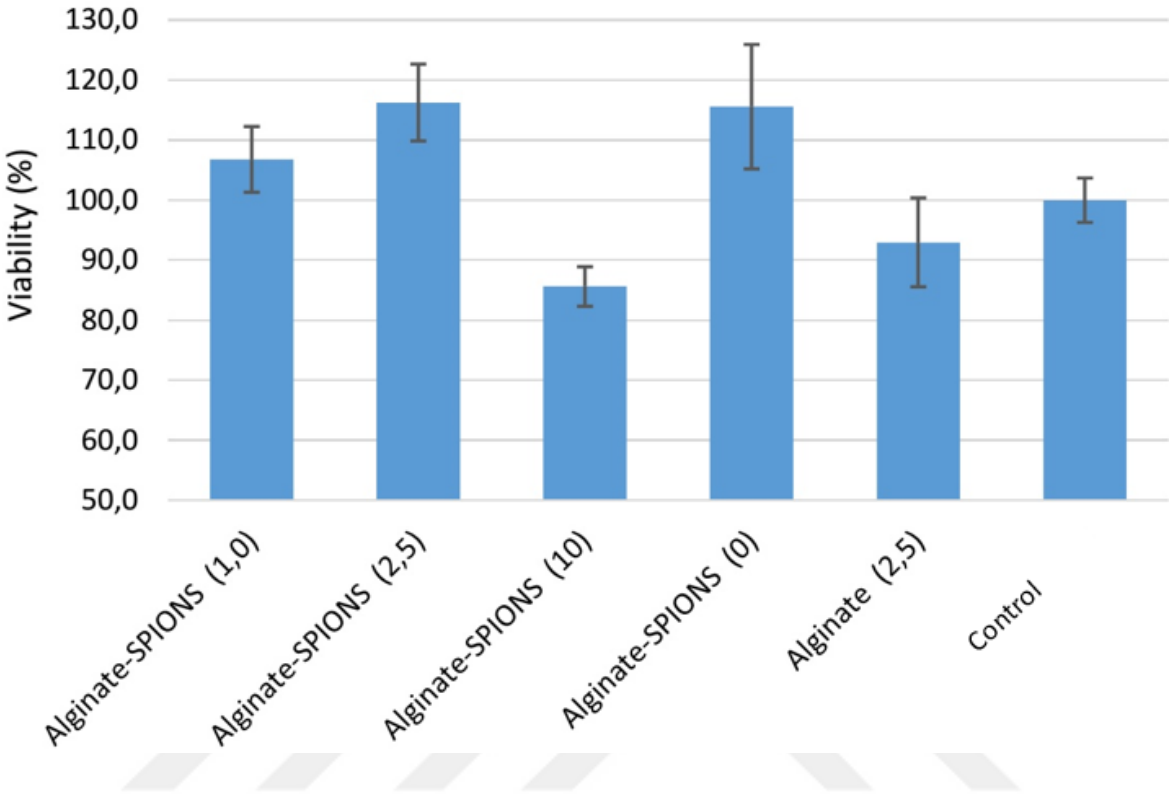

5. CONCLUSION

As a conclusion it can be stated that Sorafenib + SPION encapsulated Alginate microspheres were found to be easily formed without the need for expensive synthesis methodology and equipment. It was also found that the SPIONs were very magnetic and were produced at a size that could be efficiently used for MRI imaging in addition to hyperthermia treatment of HCC tumours.

Firstly, for the synthesis of optimally sized and shaped alginate microspheres to be possible, optimization tests were carried out changing various parameters. For producing the microspheres, the Buchi Encapsulator apparatus was used. This apparatus used the combination of frequency and electric voltage applications to generate a continuous stream of microspheres from a micro sized nozzle. Therefore, one of the parameters tested that could be changed was the frequency applied by the machine. As can be observed from the results, an application of 1600 Hz frequency was ideal. Another parameter that was tested was the concentration of the cross-linker solution ($CaCl_2$). This was to see which concentration would result in more stable and better shaped microspheres. It was found that a combination of 1600 Hz frequency with 600 mV of electric voltage applied to an 80 µm nozzle resulted in uniform and homogenous particles with the smallest size possible, while the cross linker solution that the microspheres dropped into was found to form the optimal microspheres when it had a concentration of 5%. The final size obtained from the tests were around 109 µm empty alginate microspheres.

Additionally, tests were carried out to determine the best possible way of drying the microspheres with minimal loss in shape and size. It was found that drying pure alginate microspheres without them losing their shape was not possible. Therefore, HPMC was added to the alginate solution at a ratio of 1:9 and Tween-85 was added to the Calcium Chloride cross linker solution to decrease the shear force when the alginate microspheres were hitting the cross linker solution. These formulations were found to be very affective and solid dried alginate microspheres were obtained with minimal change in shape.

The next step in the thesis was to determine the optimal method for producing super paramagnetic iron oxide nanoparticles (SPIONs) that were homogenous and had a size less than or equal to 60-70 nm. It was found that the molar ratio of the $FeCl_3.6H_2O$ iron (III) and $FeCl_2$ $4H_2O$ iron (II) salts must be at 1:2 and that the acid HCl had to be used to counteract

the surface charge of the nanoparticles which were negatively charged. For the precipitation of the Fe^{3+} and Fe^{2+} ions a solution of NaOH at a concentration of 1M was dropped slowly in to the iron salt solution. Additionally, the whole procedure was carried out under an atmosphere of nitrogen gas that was continually allowed to enter the system so as to prevent the oxidation of ions as much as possible. The obtained nanoparticles had a size of approximately 50-60 nm when measured using the Zeta Sizer.

The next step was to produce SPION Alginate microspheres. This was found to be easier to do by preparing the SPION solution first and adding it to the alginate solution in a way that produced a final concentration of 1.2% alginate. The concentration of the SPIONs were at 5 mg/ml. The SPION alginate microspheres were found to be approximately the same size as empty alginate microspheres.

For the swelling ratio calculations, the diameter of the microspheres was measured at time intervals and the equation Swelling % = D_t - D_0/D_0 x 100 was used for calculating the percentage of swelling observed in the microspheres. It was found that a higher percentage of swelling was observed in alginate microspheres containing SPIONs than those that were empty.

Morphological studies of the SPIONs using SEM images showed that they were in fact much smaller than the Zeta Sizer results showed and were closer to the size of approximately 20 nm, with the nanoparticles showing uniformity and homogeneity in size and shape. Additionally, the morphological studies of the microspheres, via photos taken from an attached camera on an optical microscope, showed them to also exhibit uniform and homogenous forms and shapes, even when they were dried. This showed that the optimization tests had been successful and resulted in microspheres that were stable and able to be used at later times.

For studying the magnetic properties of both the naked SPIONs and the SPION alginate microspheres, VSM and ESR tests were carried out. These tests showed that the SPIONs were in fact super paramagnetic and showed strong magnetism. Additionally, it was expected that the SPION alginate microspheres would have much lower magnetic properties as opposed to the naked SPIONs. However, it was observed that this difference was lower than expected and not that much difference was observed in these properties.

Hyperthermia studies were also carried out. It was observed that iron oxide and both its washed and unwashed samples were able to heat the environment and thus could be used for hyperthermia treatments.

The drug loading and release tests showed that a relatively expected curve was obtained where the drug concentration measurements showed an initial exponential release from the microspheres for the first few hours, after which it was found that the concentration of the Sorafenib drug in the environment began to level off. Finally, the concentration of the drug was found to be the same for the remainder of the measurements. Therefore, drug release studies were found to be successful and according to literature.

The MTT cytotoxicity studies showed that, as expected, those microspheres with a higher concentration of Sorafenib resulted in lower cell viability of the L292 cells as opposed to those with lower concentrations. Therefore, it can be deduced that targeting the microspheres directly on to the tumour site will be much more preferable and, due to TACE method the microspheres were designed to be used in, this will be possible.

As a conclusion, the results of this thesis show that by incorporating SPIONs and Sorafenib in alginate microspheres, a cheap and easily producible DEB was able to be produced. In addition, the implications that SPIONs give to the future of this study and those like it is immeasurable. This is due to SPIONs being able to be used as imaging agents in MRIs and their hyperthermia properties that allow tumour cells to be the only cells affected with minimal damage to surrounding healthy cells. Additionally, due to the magnetic strength of the SPIONs, they can be further developed so that they can be maneuvered via an external magnetic field and targeted directly to the tumour site.

6. REFERENCES

[1] L.J. de Oliveria Andrade, et al., Association between hepatitis C and hepatocellular carcinoma, Journal of Global Infectious Diseases, 1(1) (**2009),** 33-7.

[2] H.B. El-Serag, Epidemiology of viral hepatitis and hepatocellular carcinoma., Gastroenterology, 142(6) **(2012**),1264-1273 e1.

[3] L.P. Waller, V. Deshpande, and N. Pyrsopoulos, Hepatocellular carcinoma: A comprehensive review, World Journal Hepatology, 7(26)(**2015**), 2648-63.

[4] J. Balogh, et al., Hepatocellular carcinoma: a review, Journal of Hepatocellular Carcinoma, 3 (**2016**), 41-53.

[5] A. Raza and G.K. Sood, Hepatocellular carcinoma review: current treatment, and evidence-based medicine, World Journal of Gastroenterology, 20(15)(**2014),** 4115-27.

[6] S.W. Shin, The current practice of transarterial chemoembolization for the treatment of hepatocellular carcinoma, Korean Journal of Radiology, 10(5)(**2009**), p. 425-34.

[7] J.E. Song, and D.Y. Kim, Conventional vs drug-eluting beads transarterial chemoembolization for hepatocellular carcinoma, World Journal of Hepatology, 9(18) (**2017**), p. 808-814.

[8] Anonymous, Liver- Anatomy and Function of the Human Liver, https://www.innerbody.com/image_digeov/card10-new2.html (Cited on: **January 2019**)

[9] Anonymous Anatomy Of Liver In Body, http://didier-chantier.com/anatomy-of-liver-in-body/anatomy-of-liver-in-body-referring-web-photo-gallery-with-anatomy-of-liver-in-body/,(Cited on: **January 2019**)

[10] Anonymous, Physiology of the liver, https://anatomy-medicine.com/digestive-system/27-physiology-of-the-liver.html, (Cited on: **January 2019)**

[11] J.C. Ozougwu, Physiology of the liver, International Journal of Research in Pharmacy and Biosciences, 4(**2017**), p. 13-24.

[12] D.C. Rizzo, Fundamentals of anatomy and physiology. 4 ed, Cengage Learning, **2015.**

[13] A.S. Lok, et al., Incidence of hepatocellular carcinoma and associated risk factors in hepatitis C-related advanced liver disease., Gastroenterology, 136(1) (**2009),** 138-48.

[14] H.B. El-Serag and F. Kanwal, Epidemiology of hepatocellular carcinoma in the United States: where are we? Where do we go?, Hepatology, 60(5) (**2014)** 1767-75.

[15] S. Mittal and H.B. El-Serag, Epidemiology of hepatocellular carcinoma: consider the population, Journal of Clinical Gastroenterology, 47 Suppl: p. S2-6, **2013.**

[16] Jonathan M Schwartz and J. Robert L Carithers, Epidemiology and etiologic associations of hepatocellular carcinoma, https://www.uptodate.com/contents/epidemiology-and-etiologic-associations-of-hepatocellular-carcinoma, (Cited on: **January 2019)**

[17] K.A. McGlynn, J.L. Petrick, and W.T. London, Global epidemiology of hepatocellular carcinoma: an emphasis on demographic and regional variability. Clinical Liver Disease, 19(2) (**2015)** p. 223-38.

[18] L. Cicalese, Hepatocellular Carcinoma, https://emedicine.medscape.com/article/197319-overview (cited on: **December 2018**)

[19] M. Benedict and X. Zhang, Non-alcoholic fatty liver disease: An expanded review, World Journal of Hepatology, **2017**. 9(16): p. 715-732.

[20] F.Z. Khan et al., Advances in hepatocellular carcinoma: Nonalcoholic steatohepatitis-related hepatocellular carcinoma, World Journal of Hepatology, 7(18)(**2015**), p. 2155-61.

[21] Anonymous, Hepatocellular Carcinoma, http://www.assignmentpoint.com/science/medical/hepatocellular-carcinoma.html, (cited on: **December 2018**)

[22] A.M. Khalaf et al., Role of Wnt/beta-catenin signaling in hepatocellular carcinoma, pathogenesis, and clinical significance, Journal of Hepatocellular Carcinoma, 5 (**2018)** p. 61-73.

[23] H. Huynh, et al., Over-expression of the mitogen-activated protein kinase (MAPK) kinase (MEK)-MAPK in hepatocellular carcinoma: its role in tumor progression and apoptosis, BMC Gastroenterology, 3 (**2003)** p. 19.

[24] S.M. Wilhelm, et al., Preclinical overview of sorafenib, a multikinase inhibitor that targets both Raf and VEGF and PDGF receptor tyrosine kinase signaling, Molecular Cancer Therapeutics, 7(10) **(2008),** p. 3129-40.

[25] S. Yang and G. Liu, Targeting the Ras/Raf/MEK/ERK pathway in hepatocellular carcinoma, Oncology Letters, 13(3) **(2017),** p. 1041-1047.

[26] J.M. Llovet et al., Sorafenib in advanced hepatocellular carcinoma, The New England Journal of Medicine, 359(4) (**2008),** p. 378-90.

[27] R.C. Kane et al., Sorafenib for the treatment of advanced renal cell carcinoma. Clinical Cancer Researchearch, 12(24) (**2006**), p. 7271-8.

[28] Juergen Siepmann, Ronald A. Siegel, and M.J. Rathbone, Fundamentals and applications of controlled release drug delivery, Springer Science & Business Media, **2011.**

[29] E.P. Holowka and S.K. Bhatia, Drug Delivery: Materials Design and Clinical Perspective. **2014**.

[30] S. Vaidya, K.R. Tozer, and J. Chen, An overview of embolic agents, Seminar in Interventional Radiology, 25(3) (**2008)**, 204-15.

[31] J. Krysl and D.A. Kumpe, Embolization Agents: A Review, Techniques in Vascular and Interventional Radiology, (**2000**), p. 158-161.

[32] R. Salem and R.J. Lewandowski, Chemoembolization and radioembolization for hepatocellular carcinoma, Clinical Gastroenterology and Hepatology, 11(6)(**2013)**, p. 604-11; quiz e43-4.

[33] K.Y. Tam, K.C. Leung, and Y.X. Wang, Chemoembolization agents for cancer treatment, European Journal of Pharmaceutical Sciences, 44(1-2) (**2011)**, p. 1-10.

[34] M. Groher, 2D-3D Registration of Vascular Images - Towards 3D-Guided Catheter Interventions, **2008**.

[35] Y.X. Wang et al., Transcatheter embolization therapy in liver cancer: an update of clinical evidences, Chinese Journal of Cancer Researchearch, 27(2) (**2015)**, p. 96-121.

[36] K.Y. Lee and D.J. Mooney, Alginate: properties and biomedical applications, Progress in Polymer Science, 37(1) (**2012)**, p. 106-126.

[37] Anonymous, What is Alginate? https://www.iroalginate.com/alginate.htm, (Cited on: **2018**)

[38] H.H. Tonnesen and J. Karlsen, Alginate in drug delivery systems, Drug Development and Industrial Pharmacy, 28(6) (**2002),** p. 621-30.

[39] A. Sosnik, Alginate Particles as Platform for Drug Delivery by the Oral Route: State-of-the-Art, ISRN Pharmacology, (**2014**), p. 926157.

[40] Y.E. Choi, J.W. Kwak, and J.W. Park, Nanotechnology for early cancer detection, Sensors (Basel), 10(1) (**2010),** p. 428-55.

[41] G.A. Mansoori et al., Nanotechnology in cancer prevention, detection and treatment: bright future lies ahead, ed. P.W.L. Filho. **2007**: Inderscience Enterprises Ltd.

[42] R. Misra, S. Acharya, and S.K. Sahoo, Cancer nanotechnology: application of nanotechnology in cancer therapy, Drug Discovery Today, 15(19-20) (**2010**), p. 842-50.

[43] T. Takashima et al., Diagnosis and screening of small hepatocellular carcinomas. Comparison of radionuclide imaging, ultrasound, computed tomography, hepatic angiography, and alpha 1-fetoprotein assay, Radiology, 145(3) (**1982**), p. 635-8.

[44] M.S. Peterson and R.L. Baron, Radiologic diagnosis of hepatocellular carcinoma, Clinical Liver Disease, 5(1)(**2001**), p. 123-44.

[45] L. Bolondi et al., Surveillance programme of cirrhotic patients for early diagnosis and treatment of hepatocellular carcinoma: a cost effectiveness analysis, Gut, 48(2)(**2001**), p. 251-9.

[46] J.P. Achkar et al., Undetected hepatocellular carcinoma: clinical features and outcome after liver transplantation, Liver Transpl Surg, 4(6) (**1998**), p. 477-82.

[47] D.D. Brahee et al., Body Mass Index and Abdominal Ultrasound Image Quality: A Pilot Survey of Sonographers, Journal of Diagnostic Medical Sonography, (**2013**), p. 66–72.

[48] A. Colli et al., Accuracy of ultrasonography, spiral CT, magnetic resonance, and alpha-fetoprotein in diagnosing hepatocellular carcinoma: a systematic review, The American Journal of Gastroenterology, 101(3) (**2006**), 513-23.

[49] M.S. Martina et al., Generation of superparamagnetic liposomes revealed as highly efficient MRI contrast agents for in vivo imaging. Journal of the American Chemical Society, 127(30) (**2005**), 10676-85.

[50] S.Y. Choi et al., MRI traceability of superparamagnetic iron oxide nanoparticle-embedded chitosan microspheres as an embolic material in rabbit uterus, Diagnostic and Interventional Radiology, 21(1) (**2015**), 47-53.

[51] E.Y. Chung et al., Design of deformable chitosan microspheres loaded with superparamagnetic iron oxide nanoparticles for embolotherapy detectable by magnetic resonance imaging. Carbohydrate Polymers, 90(4) (**2012**), 1725-31.

[52] H.S. Lee et al., Synthesis of SPIO-chitosan microspheres for MRI-detectable embolotherapy, Journal of Magnetism and Magnetic Materials, (**2005**), 102–105.

[53] R. Cilliers, et al., Modification of embolic-PVA particles with MR contrast agents, Magnetic Resonance in Medicine, 59(4) (**2008**), 898-902.

[54] Z. Yuan, et al., Role of magnetic resonance diffusion-weighted imaging in evaluating response after chemoembolization of hepatocellular carcinoma, European Journal of Radiology, 75(1)(**2010**), e9-14.

[55] A. Mayer, et al., The role of nanoparticle size in hemocompatibility, Toxicology, 258(2-3) (**2009**), 139-47.

[56] C.H. Yu, et al., Immobilization of BSA on Silica-Coated Magnetic Iron Oxide Nanoparticle, The Journal of Physical Chemistry, (**2009**), 537–543.

[57] X. Yu, et al., A Facile Approach to Fabrication of Bifunctional Magnetic-Optical Fe3O4@ZnS Microspheres, Chemistry of Materials, (**2009)**, 4892–4898.

[58] Y. Liu, et al., An efficient colorimetric biosensor for glucose based on peroxidase-like protein-Fe3O4 and glucose oxidase nanocomposites, Biosensors and Bioelectronics, 52(**2014),** 391-6.

[59] X. Chenjie, et al., *A*u–Fe3O4 Dumbbell Nanoparticles as Dual-Functional Probes**, Angew Chem Int Ed Engl, (**2008**), 173 –176.

[60] K. Hayashi, et al., High-frequency, magnetic-field-responsive drug release from magnetic nanoparticle/organic hybrid based on hyperthermic effect, ACS Applied Materials & Interfaces, 2(7) (**2010**), 1903-11.

[61] W. Chen, et al., Composites of aminodextran-coated Fe3O4 nanoparticles and graphene oxide for cellular magnetic resonance imaging, ACS Applied Materials & Interfaces, 3(10)(**2011**), 4085-91.

[62] H. Fukao, et al., Effect of hyperthermia on the viability and the fibrinolytic potential of human cancer cell lines, Clinica Chimica Acta, 296(1-2) (**2000**), 17-33.

[63] F.K. Storm, et al., Normal tissue and solid tumor effects of hyperthermia in animal models and clinical trials, Cancer Research, 39(6 Pt 2) **(1979),** 2245-51.

[64] E.J. Hall and A.J. Giaccia, Radiobiology for the Radiologist, 6 ed., Lippincott Williams and Wilkins Publishing, **2006.**

[65] D. Jain and D. Bar-Shalom, Alginate drug delivery systems: application in context of pharmaceutical and biomedical research, Drug Development and Industrial Pharmacy, 40(12)(**2014),** 1576-84.

[66] M. van Elk, et al., *A*lginate Microspheres Containing Temperature Sensitive Liposomes (TSL) for MR-Guided Embolization and Triggered Release of Doxorubicin, PLoS One, 10(11)(**2015),** e0141626.

[67] M. Szekalska, A. Amelian, and K. Winnicka, Alginate microspheres obtained by the spray drying technique as mucoadhesive carriers of ranitidine, Acta Pharmaceutica, 65(1) **(2015**), 15-27.

[68] E. Tombacz, et al., Magnetic iron oxide nanoparticles: Recent trends in design and synthesis of magnetoresponsive nanosystems. Biochemical and Biophysical Research Communications, 468(3)(**2015),** 442-53.

[69] S. Laurent, et al., Magnetic iron oxide nanoparticles: synthesis, stabilization, vectorization, physicochemical characterizations, and biological applications. Chemical Reviews, 108(6)(**2008**), 2064-110.

[70] N. D. Kandpal, et al., Co-precipitation method of synthesis and characterization of iron oxide nanoparticles, Journal of Scientific&Industrial Research, **(2014)** p. 87-90.

[71] R. Massart, Preparation of Aqueous Magnetic Liquids in Alkaline and Acidic Media, IEEE Transactions on Magnetis, (**1981**)

[72] Q. Wang et al., Magnetic alginate microspheres detected by MRI fabricated using microfluidic technique and release behavior of encapsulated dual drugs, International Journal of Nanomedicine, 12(**2017),** 4335-4347.

[73] G. Germanos, et al., Diffusion and agglomeration of iron oxide nanoparticles in magnetic calcium alginate beads initiated by copper sorption, (**2017**)

[74] A. Grillone, et al., Active Targeting of Sorafenib: Preparation, Characterization, and In Vitro Testing of Drug-Loaded Magnetic Solid Lipid Nanoparticles, Advanced Healthcare Materials, 4(11) (**2015),** 1681-90.

[75] J. Chen, et al., Poly(lactide-co-glycolide) microspheres for MRI-monitored transcatheter delivery of sorafenib to liver tumors, Journal of Controlled Release, 184 (**2014**), 10-7.

[76] C. Sultana, Formulation and Evaluation of Sorafenib Tosylate Immediate Release Tablets, Masters Thesis, Adhiparasakthi College of Pharmacy, India, **2012**.

[77] M. Bongardt, Microencapsulation of doxycycline with alginate and HPMC and its effect on drug stability, Masters Thesis, University of Iceland, Iceland, **2014**.

HACETTEPE UNIVERSITY
GRADUATE SCHOOL OF SCIENCE AND ENGINEERING
THESIS / DISSERTATION ORIGINALITY REPORT

HACETTEPE UNIVERSITY
GRADUATE SCHOOL OF SCIENCE AND ENGINEERING
TO THE DEPARTMENT OF BIOENGINEERING

Date: 29/01/2019

Thesis Title / Topic: DEVELOPMENT AND CHARACTERISATION OF MAGNETICALLY RESPONSIVE AND ACTIVE AGENT LOADED ALGINATE BASED MICROSPHERES TO BE USED IN THE TREATMENT OF HEPATOCELLULAR CARCINOMA (HCC)

According to the originality report obtained by myself by using the *Turnitin* plagiarism detection software and by applying the filtering options stated below on 16/01/2019 for the total of 70 pages including the a) Title Page, b) Introduction, c) Main Chapters, d) Conclusion sections of my thesis entitled as above, the similarity index of my thesis is 4 %.

Filtering options applied:

1. Bibliography/Works Cited excluded
2. Quotes excluded / ~~included~~
3. Match size up to 5 words excluded

I declare that I have carefully read Hacettepe University Graduate School of Science and Engineering Guidelines for Obtaining and Using Thesis Originality Reports; that according to the maximum similarity index values specified in the Guidelines, my thesis does not include any form of plagiarism; that in any future detection of possible infringement of the regulations I accept all legal responsibility; and that all the information I have provided is correct to the best of my knowledge.

I respectfully submit this for approval.

29/01/2019
Date and Signature

Name Surname:	Şükran Alpdemir
Student No:	N15220343
Department:	Bioengineering
Program:	Masters in Bioengineering
Status:	☒ Masters ☐ Ph.D. ☐ Integrated Ph.D.

ADVISOR APPROVAL

APPROVED.

Prof. Dr. Emir Baki Denkbaş

CURRICULUM VITAE

Name Surname : Şükran Alpdemir

Place of Birth : Yenimahalle, Ankara

Date of Birth : 18.08.1991

Marital Status : Single

Address : Batıkent, Yenimahalle, Ankara

Email : shukranalpdemir@gmail.com

Languages : Turkish, English, Bosnian, French

EDUCATION

BSc : International University of Sarajevo- Genetics and Bioengineering (2010-2014)

Work Experience

2018- TUBITAK UIDB

Areas of Experiences : Nanotechnology and drug targeting, bioinformatics

PUBLICATIONS

Mohamed Ragab Abdel Gawwad, Şükran Alpdemir, Edina Eminagic, Interactome Analysis and Docking Sites of PCNA Subunits Reveal New Function in Arabidopsis thaliana, Current Proteomics 12(3):152-167, November 2015